LOW-RANK COAL LIQUEFACTION H-DONOR STUDIES USING ^2H NMR

S.A. Farnum, B.W. Farnum, J.R. Rindt, D.J. Miller, and A.C. Wolfson

University of North Dakota
Energy Research Center
Box 8213, University Station
Grand Forks, North Dakota 58202

Several batch autoclave experiments were carried out using natural abundance 30.7 MHz ^2H NMR spectroscopy of product fractions to assess H-donor activity during lignite liquefaction. ^2H NMR observations of deuterium enrichments and measurement of ^2H NMR distributions have been used to investigate liquefaction reactions (1-3).

The development of high field superconducting magnets that operate in the Fourier transform mode with high sensitivity probes has made it possible to monitor liquefaction reactions by natural abundance ^2H NMR (0.0156% natural abundance). It is, therefore, no longer necessary to add large amounts of deuterated solvents or even large amounts of deuterated H-donors which swamp out critical aspects of the liquefaction reaction. The use of natural abundance ^2H NMR allows the investigator to examine typical liquefaction reactions without disturbing the system by the addition of large amounts of extraneous materials.

Martin et al. demonstrated recently that very important and often very spectacular variations may be found in the internal distribution of deuterium within molecules (4, 5). Measurement of the naturally abundant ^2H NMR distribution may be used to provide valuable information on the selectivity of ^2H repartition. Martin et al. applied measurements of this type to determine the origin of natural products such as alcohols in which samples from various sources with different histories had different ^2H NMR distributions (4).

It may be inferred from the work of Cronauer et al (6) and of Brower (7), that the method of Martin may be applied to the investigation of the reactions of H-donors during coal liquefaction. Brower (7) reported that the H/D kinetic isotope effect for the reaction of coal with tetralin containing deuterium at the alpha positions is 2.1 ± 0.1 at 335°C. The reaction mixture was 1 g of deuterated or undeuterated tetralin with 1 g of subbituminous coal in glass ampules. Rates of reaction were compared by monitoring the naphthalene/tetralin ratios.

When Cronauer (6) carried out liquefaction of Powhatan No. 5 coal in 100% 1,2,3,4-d_4-tetralin solvent and in 100% d_{12}-tetralin, he also showed clearly that the abstraction of ^1H from a hydroaromatic carbon having one ^2H and one ^1H substitutent is greatly preferred. Since the natural abundance of ^2H is only 0.015%, the probability that a carbon would have two ^2H substituents is very, very small. It is therefore possible to use the natural system as an *in situ* probe for comparing reactivities of H-donors under actual liquefaction conditions.

If reactions occur which involve a hydroaromatic carbon, and ^1H is preferentially abstracted each time, the ^2H distribution will show an increase in that spectral region. If a large amount of H-donor activity in the regions α and β to aromatic rings (H_α and H_β) occurs during liquefaction, the ^2H distribution should reflect this by showing a corresponding increase in the 5.0 - 1.8 ppm region of the natural abundance ^2H NMR spectrum.

Since the natural abundance ^2H NMR spectrum reflects the reactive history of the sample, adequate blank experiments must be performed to determine original or non-affected ^2H distributions. They always differ from the proton NMR distributions

when the sample has reactive history that involved H-transfer reactions. Since we used a process coal-derived liquid as our solvent, the blank autoclave run was essential.

Another aspect of liquefaction involves the interaction of processing gases with the solvent or directly with the coal or coal fragments. This question has been addressed by several investigators (1, 3, 8, 9, 10). The types of molecules that are active during liquefaction either through exchange reactions, through hydrogenation, hydrogen transfer, or through direct reaction with H_2 gas may be inferred by substituting deuterium gas $^2H_2$ for the H_2 in the reactive gas mixture. The reactive sites are then located by ^2H NMR of the enriched reaction mixture.

Experimental

Autoclave experiments were designed to simulate processing conditions in our continuous process bottoms recycle liquefaction unit.

The experiments were carried out in a 1-liter hot-charged autoclave (11). The coal (65 g maf) solvent (120 g) slurry was hot-charged into the preheated autoclave, reaching the operating temperature of 450°C in less than two minutes. The reactant gas (40 g, unlabeled) was 50/50 H_2/CO or $^2H_2/CO$ at a pressure of 3700 psig under reaction conditions. Residence time was 20 minutes after which the entire contents of the autoclave were transferred into a quench vessel, cooled and depressurized at room temperature. Gases were analyzed and the product slurry was distilled (ASTM D-1160). The trap contents (mainly water), the ASTM D-1160 distillate, and vacuum bottoms were subjected to separations and NMR analyses.

Mass balances were obtained using a different portion of the slurry and analyzing it for water, ash, tetrahydrofuran (THF) solubility, and vacuum distillate at 5 torr. The additive, when used, was 1,2,3,4-tetrahydrophenanthrene (THPhen) (0.33 g). The run matrix is shown in Table I.

TABLE I

AUTOCLAVE TESTS WITH BIG BROWN LIGNITE, RECYCLE SLURRY DISTILLATE, 450°C and 3400-3700 PSI TOTAL PRESSURE

Run No.	Processing Gas	Additive
3	H_2/CO	None
4	H_2/CO	THPhen
5	$^2H_2/CO$	THPhen

The coal and solvent chosen for these tests were a Texas lignite from the Big Brown mine and a recycle slurry ASTM D-1160 distillate from a continuous processing unit (CPU) run carried out at UNDERC using the same coal. The solvent was distilled from slurry collected on the thirteenth bottoms recycle pass. A cold trap was used during distillation to assure the collection of all volatile oils and water.

The ASTM D-1160 distillate of the autoclave product was further separated into alkanes, aromatics, and polars by open column chromatography on neutral silica gel with pentane, methylene chloride, and methanol as elution solvents. The fractions were cleanly separated as shown by examination of their 200 MHz ^1H NMR spectra. The vacuum bottoms (10 g) were Soxhlet extracted with refluxing $CHCl_3$ (500 ml) for 20 hours, followed by THF (500 ml) for 20 hours. The residue consisting of inorganic

material, insoluble organic matter and unreacted coal amounted to 65-70% of the vacuum bottoms. Chloroform extracted 25-30% while the remainder of 3-4% was extracted with THF.

NMR spectra were obtained at 200 MHz in CD_2Cl_2 for protons and at 50.3 MHz in $CDCl_3$ for ^{13}C using pulsing conditions appropriate to the sample. ^2H NMR spectra were pulsed at 30.7 MHz 1-30,000 times depending on the sample. A 45° flip angle was used with an acquisition time of 4 seconds and a delay of 4 seconds. The solvent used was methylene chloride, CH_2Cl_2.

^2H enrichments of the fractions from Experiment 5 were determined by standard addition of CD_2Cl_2 to a preweighed oil sample. The standard addition line gave a linear regression value of r = 0.993. The sample was weighed tightly covered and diluted immediately with CH_2Cl_2. The enrichment of the water samples from the distillation trap was determined directly against a standard D_2O in H_2O curve whose linear regression value of r was 0.9999.

RESULTS AND DISCUSSION

Effect of Added H-Donor

Test numbers 3 and 4 were identical except that a small amount of an H-donor, THPhen, was added to Test 4 (Table I). Total percent conversion was essentially the same for Runs 3 and 4 (72%, 70%). Conversions to THF solubles were 56% and 60%, respectively.

The 50 MHz ^{13}C spectra for the light oils, the distillable oils, and their fractions and the $CHCl_3$ soluble vacuum bottoms were very similar for Runs 3 and 4. The 200 MHz ^1H NMR spectra of the products were likewise indistinguishable from run to run with corresponding fractions showing the same spectral features.

The natural abundance 30.7 MHz ^2H NMR distributions are, however, quite different from each other for the autoclave tests with and without the addition of small amounts of the H-donor, THPhen (Table II). These differences are mainly seen in the alpha + beta and in the aromatic regions of the spectrum (Figure 1). The change in the alpha + beta region gave a run 4/run 3 ratio of 1.25, clearly indicating increased H-transfer activity during Run 4.

TABLE II

^2H NMR AREA DISTRIBUTIONS FOR AUTOCLAVE TEST
WITH BIG BROWN TEXAS LIGNITE, H_2/CO, 450°C, MPa (3700 PSI)

	Run 3 (Area %)	Run 4 (Area %)	Run 4/3 (Area %)
Aromatic (9.6 - 5.8 ppm)	39.7	45.9	1.16
Alpha + Beta (5-1.8 ppm)	28.6	35.7	1.25
Other (1.8-0.1 ppm)	31.6	19.4	0.61

To test the effect of H-donor addition without liquefaction reaction, two portions of liquefaction recycle solvent distillate were equilibrated for three weeks at room temperature with and without the addition of the same amount of H-donor. When compared by ^2H NMR spectroscopy, there was no change in ^2H distribution.

The change in the ^2H distribution under liquefaction conditions therefore may be attributed to an increased cumulative isotope effect during liquefaction with small amounts of added H-donor. The small increase in THF soluble product, 60% as compared with 56% may be related to the H-donor activity increase but is not as notable during autoclave testing as it would be in CPU recycle operation.

Processing with $^2H_2/CO$

Autoclave Test 5 was conducted with deuterium-labeled 50/50 $^2H_2/CO$ and added THPhen. A deuterium-enriched product was obtained. Total conversion was 67% and conversion to THF solubles was 50%. The 50% conversion of lignite to THF solubles in Run 5 processed with $^2H_2/CO$ is significantly lower than the 60% conversion in Run 4 processed with $^1H_2/CO$. The deuterium isotope effect resulting from the use of $^2H_2$ rather than $^1H_2$, in the gas mixture would be expected to lower the yield of THF solubles since the rate of reaction of $^2H_2$ is expected to be slower than the rate of reaction of $^1H_2$ (7).

Examination of the product by ^2H NMR using the methods described in the Experimental section showed that ^2H entered every fraction of the product, including the H_2O, the ASTM distillate, and the soluble vacuum bottoms (Table III). The water was the most highly enriched fraction, probably due to the easy exchange of water hydrogens with the $^2H_2$ gas. Other hydrogens expected to exchange rapidly with $^2H_2$ gas are those ortho and para to phenolic OH groups and methylene hydrogens alpha and beta to aromatic rings. The fractions (polars, aromatics, ASTM D-1160 dist.) containing these types of bonds show appreciable enrichment (Table III). In the case of the aromatic fraction (Figure 2), it is even possible to assign some of the most exchangeable hydrogens to specific compounds. For example, the peaks at 3.9 ppm and 3.6 ppm in the proton NMR spectrum (Figure 2, top) can be plainly seen as enriched peaks in the deuterium NMR spectrum (bottom). These peaks are assigned to the methylene hydrogens of fluorene and acenaphthene respectively. It is notable that very little enrichment or exchange occurs on terminal methyl carbons of alkyl chains (0.9 ppm); however, the methylene region (~1.2 ppm) is enriched.

TABLE III

PRODUCTS FROM AUTOCLAVE TEST 5 (BIG BROWN TEXAS LIGNITE, $^2H_2/CO$, 450°C, 3400 PSIG), DETERMINED BY ^2H NMR

Product	No. Grams in Product	Wt % ^2H	Wt % H in Sample	*Enrichment Factor
Water	29.31	2.62	11.11	760
ASTM D-1160 Distillate	109.4	0.606	7.17	270
Fraction of Distillate:				
Alkanes	11.4	0.58 (by diff.)	14.88	120
Aromatics	44.9	0.542	7.20	240
Polars	30.9	0.967	7.81	400
ASTM D-1160 $CHCl_3$ Soluble Bottoms	25.74	0.605	5.84	330

$$* \quad \frac{\text{atom \% } ^2H}{0.0156\% \text{ (Natural Abundance)}}$$

Figure 3 shows the comparison of the ASTM D-1160 distillate polar fraction 200 MHz ^1H NMR spectrum (top) and the 30.7 MHz ^2H NMR spectrum (bottom). The aromatic region of the ^2H spectrum was more enriched than the rest of the spectrum.

Since considerable amounts of ^2H (about 35 wt. % of the $^2H_2$ added) entered the product, it is impossible to assign any of the incorporated ^2H to reaction product rather than exchange product. However, it is possible to note that some portions of the product that were enriched are materials that do not undergo exchange easily. The ^2H NMR spectrum of the alkanes separated from the ASTM D-1160 distillate shows incorporation of deuterium into both methylene and methyl regions of the spectrum and the overall enrichment of the alkane fraction is ~120 x natural abundance.

The most actively enriched portions of the alkanes, aromatics, and polars may be seen by comparing Autoclave Run 4 (H_2/CO) with Run 5 ($^2H_2$/CO), Table IV and to compare ASTM D-1160 distillate oils, Table V.

Summary

1. Differences in natural abundance ^2H NMR distributions resulted from differences in the processing history of the samples.

2. The addition of small amounts of H-donor to a liquefaction reaction changed the natural abundance ^2H NMR distribution with respect to an identical run without added donor. The ^1H distribution and ^{13}C distribution were unchanged. Changes were probably the result of increased hydrogen transfer activity and the cumulative deuterium isotope effects.

3. Tests made using $^2H_2$/CO showed product incorporation of ^2H to >270 times the natural abundance as determined by standard addition ^2H NMR. The ^2H distribution was not the same as in the unlabeled test.

4. ^2H entered all fractions of the product during the test with $^2H_2$/CO, including ASTM distillate alkanes, phenols and polars, H_2O and soluble vacuum bottoms. Polars and H_2O were the most enriched fractions, probably due to easy H-exchange.

5. Processing with $^2H_2$/CO resulted in decreased conversion to THF solubles when compared with an identical run with $^1H_2$/CO.

Acknowledgments

UNDERC carried out this work for the U.S. Department of Energy under Cooperative Agreement No. DE-FC21-83FE-60181.

TABLE IV

^2H NMR AREA PERCENTAGES OF SEPARATED FRACTIONS OF RUN 4 AND RUN 5 PRODUCT ASTM-1160 DISTILLATE

Integrated Area %, Column Fractions, ASTM Distillate		Run 4	Run 5	Run 5/4
Alkanes	^2H_o	100.0	100.0	N/A
Aromatics	$^2H_{ar}$	50.0	35.8	0.72
	$^2H_{\alpha+\beta}$	39.3	51.1	1.31
	^2H_o	10.7	13.1	1.19
Polars	$^2H_{ar}$	33.8	43.2	1.28
	$^2H_{\alpha+\beta}$	50.2	42.9	0.85
	^2H_o	16.0	13.9	0.87

TABLE V

COMPARISON OF RESULTS WITH LABELED AND UNLABELED SYNGAS ($CO/^2H_2$), (CO/H_2), ^1H NMR AREA PERCENTAGES, ^2H NMR AREA PERCENTAGES

Integrated Area, % ASTM D-1160 Distillate	Run 4 (unlabeled)	Run 5 (labeled)	Run 5/Run 4
$^1H_{ar}$	37.7	35.0	0.93
$^1H_{\alpha+\beta}$	31.4	34.3	1.09
^1H_o	30.9	29.9	0.97
$^2H_{ar}$	45.9	43.7	0.95
$^2H_{\alpha+\beta}$	35.7	43.1	1.21
^2H_o	19.4	13.2	0.68

REFERENCES

1. Frantz, J.A. and D.M. Camaioni. Amer. Chem. Soc., Div. Fuel Chem. Preprints, 1981, 26 (1), 105-113.

2. Ratto, J.J., L.A. Heredy, and R.P. Skrowronski. Amer. Chem. Soc., Div. Fuel Chem. Preprints, 1979, 24 (2), 155-165.

3. Heredy, L.A., R.P. Skowronski, J.J. Ratto, and I.B. Goldberg. Amer. Chem. Soc., Div. Fuel Chem. Preprints, 1981, 26 (1), 114-122.

4. Martin, G.J., M.L. Martin, F. Mabon, M.J. Michon. Anal. Chem., 1982, 54, 2380-2382.

5. Martin, G.J., M.L. Martin, F. Mabon, and J. Bricout. J. Am. Chem. Soc., 1982, 104, 2658-2659.

6. Cronauer, D.C., R.I. McNeil, D.C. Young, and R.G. Ruberto. Fuel, 1982, 61, 610-619.

7. Brower, K.R. J. Org. Chem., 1982, 47, 1889-1893.

8. Schweighardt, F.K., B.C. Bockrath, R.A. Friedel, and H.L. Retcofsky. Fuel, 1976, 1254-1255.

9. Skowronski, R.L., L.A. Heredy, and J.J. Ratto. Amer. Chem. Soc., Div. Fuel Chem. Preprints, 1978, 23 (4), 155-160.

10. Wilson, M.A., P.J. Collin, P.F. Barron, and A.M. Vassallo. Fuel Proc. Technol., 1982, 5, 281-298.

11. Rindt, J.R., D.E. Severson, and A.M. Souby. "UND Hot-Charged Time-Sampled Batch Autoclave System," presented April 1980, AIChE Conf., Philadelphia, PA.

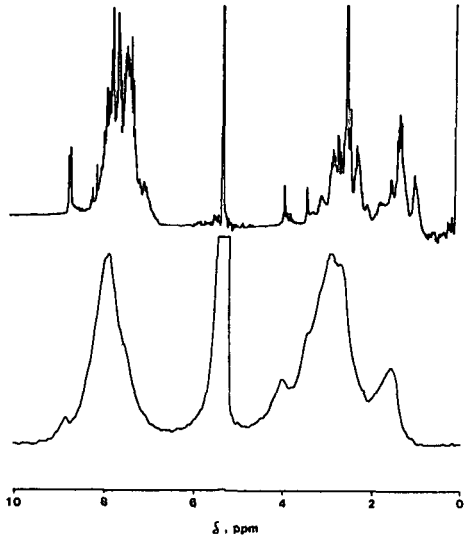

FIGURE 2. ^{1}H NMR spectrum (top) and ^{2}H NMR spectrum of the aromatic fraction of autoclave Test 5 with Big Brown Texas lignite and $^{2}H_2/CO$.

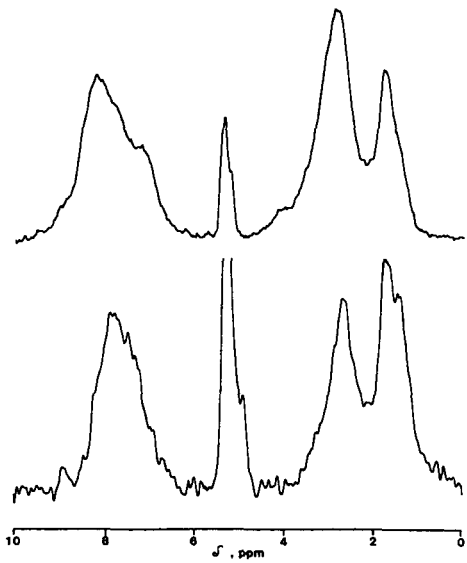

FIGURE 1. ^{2}H NMR spectra of (top) Run 4 (with added THPhen) and (bottom) Run 3 (without THPen). The peak at 5.2 ppm is the NMR solvent, CH_2Cl_2 (top) and CH_2Cl_2 with added CH_2Cl_2-d_2 (bottom). The aromatic region is designated as 9.6-5.8 ppm, the α and β region as 5.0 to 1.8 ppm and other region as 1.8 to 0.1 ppm.

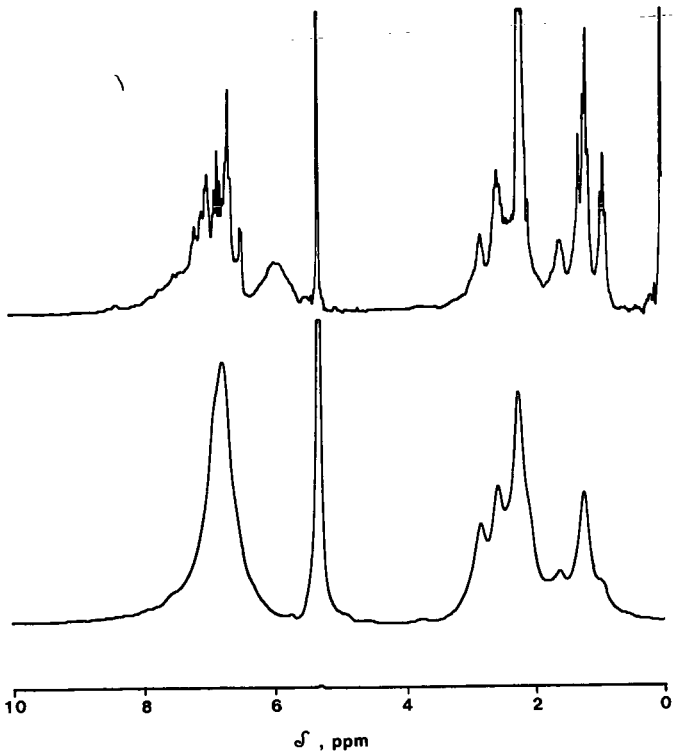

FIGURE 3. ^{1}H NMR spectrum (top) and ^{2}H NMR spectrum (bottom) of the polar fraction of autoclave Test 5 with Big Brown Texas lignite and $^{2}H_2/CO$.

INFERENCE OF SUBBITUMINOUS COAL STRUCTURE FROM LIQUEFACTION OF WYODAK COAL IN MODEL SOLVENTS*

Thomas D. Padrick and Steven J. Lockwood
Sandia National Laboratories
Albuquerque, New Mexico 87185

Introduction

Knowledge of the structure of coal is necessary if we are to understand coal liquefaction mechanisms and develop novel process concepts. Two important aspects of coal structure are the detailed structure of coal fragments and the nature of the bonds which hold these fragments together (crosslinks), the latter being the most significant to mechanism studies. The most widely accepted model for coal is that reported by Green, et al.[1] Their model consists of a macromolecular three-dimensional network of aromatic "clusters", crosslinked through covalent bonds. In their model, hydrogen bonds play a secondary role, forming only weaker bonds between molecular planes. We shall present evidence in this paper that indicates that hydrogen bonds are the primary bonds holding Wyodak coal fragments together. Evidence also suggest that hydrogen bonds are important in bituminous coal structure,[2,3] but this will not be discussed here.

Information about the nature of the crosslinks in coal has been obtained by observing the interaction of various solvents with coal. Much of the information for the model of coal presented by Green, et al. was obtained from coal swelling experiments.[4] Pampuch[5] demonstrated that the specific interaction between polar liquids and coal is the formation of hydrogen bonds. Also, several recent studies have focused on the depolymerization of coal through direct solvent attack. Larsen, et al.[6] observed depolymerization of three coals in pyridine at 350°C. The exact nature of the coal-solvent interaction was not described. Larsen[7] has also observed depolymerization of Illinois No. 6 coal in aliphatic amine bases at 300°C.

We have studied the interaction behavior of Wyodak subbituminous coal with a variety of model solvents to better understand the nature of the crosslinks in subbituminous coal. We have observed extensive depolymerization of Wyodak coal under low severity conditions, and propose that this depolymerization is the result of disruption of hydrogen bonds in the coal.

Experimental

The data reported below were obtained from batch microreactor runs using Wyodak coal (South Pit Mine) and selected model solvents. The proximate and ultimate analysis of the Wyodak coal are listed in Table 1. The solvents were all used as received from the manufacturer at the stated purity level. The 35 cm^3 microreactors were loaded with an 8 gram sample of a 2/1 solvent to coal mixture. They were then pressurized to 1000 psig with either

* This work supported by the U. S. Dept. of Energy at Sandia National Laboratories under Contract No. DE-AC04-76DP00789.

hydrogen or nitrogen. A few solvents were used in experiments at higher solvent to coal ratios to see if solvent volatilization was a problem under our conditions. Negligible differences in conversions indicate that at 375°C and a 1000 psig cold charge, solvent volatilization does not lower the solvent to coal ratio enough to alter our results. The microreactors were heated (∿3 minutes to reach reaction temperature) in a fluidized sand bath and held at temperature for the specified time. The microreactors were then cooled (∿30 seconds for a 200°C quench) in a second fluidized sand bath held at room temperature. Conversion to THF soluble products was obtained by subsampling the whole liquid product from the microreactor, sonicating the sample in THF and then pressure filtering through a 0.2 micron Milipore filter. The filtrate was then analyzed by gel permeation high performance liquid chromatography (HPLC) to observe differences in product distributions.[8] This technique separates the filtrate into high, intermediate, and low molecular weight fractions. These fractions are comparable to the classical preasphaltne (mw ∿ 1000), asphaltene (mw ∿ 450) and oil (mw ∿ 250) fractions obtained by Soxhlet analysis.[8]

Capillary GC analysis was performed on an HP 5800 using a crosslinked 5% phenyl methyl silicone column. The oven temperature was programmed from 100°C to 250°C at 2°C/min. The carrier gas flow rate was 0.5 cm^3/minute. Separated products were identified by a flame ionization detector. Product molecules as large as four and five member ring compounds have been identified by the above GC analysis technique. However, we cannot be certain all THF soluble material passed through the GC column.

Results and Discussion

We began our investigation of Wyodak coal liquefaction in model solvents by conducting experiments in tetrahydroquinoline (THQ). THQ has been observed to enhance coal conversion[3] and also to adduct to coal products.[9] Thus our initial investigation centered on learning if the same characteristic of THQ was responsible for both adduct formation and enhanced conversion. THQ is both a basic nitrogen compound and a hydrogen donor. While its basic characteristic is probably responsible for adduct formation, it is unknown which property contributes most to the enhanced coal conversions observed in THQ.

Figure 1 tabulates the conversions to THF soluble products and the product distributions for Wyodak coal liquefied at 375°C, 20 minutes and 1000 psig H_2 in 1,2,3,4-THQ, quinoline and 5,6,7,8-THQ. Quinoline is a non-hydrogen donor and shows only 23% conversion compared to 80% conversion for 1,2,3,4-THQ and 58% conversion for 5,6,7,8-THQ. In addition to being a non-hydrogen donor, the nitrogen group in quinoline is a teriary amine rather than a secondary amine as in 1,2,3,4-THQ. The 5,6,7,8-THQ should have similar hydrogen donor characteristic as the 1,2,3,4-THQ, but the conversion is much lower. The apparent difference between the two hydrogenated quinolines is that 5,6,7,8-THQ has the same base structure as quinoline.

For comparison, we measured the conversion of Wyodak coal in conventional hydrogen donor solvents, such as tetralin, hexahydropyrene and dihydrophenanthrene. Figure 2 shows the results for these three solvents. While some slight differences are observed, Wyodak conversion to THF soluble products in a good hydrogen donor solvent is 55-60% at these low severity conditions.

This is the same level of conversion that was observed for 5,6,7,8-THQ. Apparently, in 5,6,7,8-THQ only the hydrogen donor characteristic contributes to the observed conversion, i.e., there is little contribution from the quinoline type nitrogen structure. If 5,6,7,8-THQ and 1,2,3,4-THQ are similar hydrogen donors, this data would suggest that the enhanced conversion observed in 1,2,3,4-THQ is a result of the secondary amine structure.

We next conducted experiments in other basic solvents, which did not possess hydrogen donor characteristics. This was done to clarify the role of the basic functionality. Figure 3 shows the results of three liquefaction runs made in benzofuran, indole and acridine. We measured a 62% conversion for Wyodak coal liquefied in indole. Conversions in acridine and benzofuran were quite low. The high conversion in indole, a non-donor solvent, suggests a strong interaction between the coal and the basic nitrogen functionality.

The HPLC spectra from the experiments with several basic nitrogen solvents showed a new peak in the product distribution. Figure 4 illustrates the appearance of this new molecular weight peak. We see that a small complex observed with 1,2,3,4-THQ has grown to be a predominant peak in the molecular weight distribution of the THF soluble filtrate from Wyodak liquefaction in indole. We propose that this new peak is the result of an association between solvent and coal molecules.

Using preparatory-scale HPLC, we isolated samples corresponding to the new peaks shown in Figure 4. Since the complex peak occurs near the asphaltene peak, we assumed that the molecular weight of the isolated samples was approximately 400 amu. Knowing the elemental composition of indole, Wyodak coal and the isolated samples, and assuming a uniform elemental distribution for the coal, allowed us to conclude that the isolated samples contained approximately 60% indole. This result is consistent with a complex composed of two indole molecules and one coal molecule. The coal molecule would have a molecular weight of approximately 160 amu if the elemental distribution of Wyodak coal is assumed. Such a complex would have a molecular weight of $\sim$394 amu, in excellent agreement with the value of $\sim$400 amu observed for the isolated samples. Thus, our elemental analyses, in conjunction with the location of the complex peak in the HPLC molecular weight spectrum, are consistent with a complex composed of two indoles to one $\sim$160 amu coal molecule.

If the indole-coal complex is held together by hydrogen bonds, a stronger base should displace the indole from the complex. We refluxed a portion of the complex in dibutylamine at $\sim$150°C for 2 hours. Capillary GC of the complex before and after refluxing showed striking differences. Before reaction with dibutylamine, the capillary GC spectrum had only two major peaks at very long retention time. Following the dibutylamine reflux, a large peak for free indole was detected and several new peaks appeared at intermediate retention times. The major peaks previously associated with the complex were nearly eliminated. This indicates that the coal-indole complex was bound together through associative hydrogen bonds.

Indole may participate in a hydrogen bond as either an electron-acceptor or a electron-donor by virtue of the N-H group. However, since the unshared electron pair on the nitrogen participates in the ring resonance, we would expect indole to be a poor electron donor. We tested the hydrogen bonding role of indole by liquifying Wyodak in 1-methylindole. With this solvent, in which the hydrogen on the nitrogen has been replaced by a methyl group,

the solvent cannot act as an electron-acceptor in the formation of hydrogen bonds. Table 2 lists the conversion results and structural differences for indole and methylindole. Besides the dramatic decrease in Wyodak conversion, HPLC spectra indicate very little complex formation for liquefaction in methylindole. These results indicate that indole acts primarily as an electron-acceptor in hydrogen bond formation and that loss of hydrogen bonding ability of the solvent severely reduces the Wyodak conversion.

The initial experiments were performed under 1000 psig hydrogen. If indole is solubilizing coal through disruption of coal-coal hydrogen bonds and formation of coal-indole hydrogen bonds, then there should be no hydrogen consumption. We measured the % conversion to THF soluble products for a poor solvent (quinoline) and indole under both hydrogen and nitrogen pressure. Conversions for quinoline and indole were virtually the same under either reacting atomsphere. This suggests little or no hydrogen consumption from the gas phase, despite the lack of hydrogen available from either solvent.

At 375°C, there is sufficient thermal energy for some bond rupture, both covalent bonds and hydrogen bonds. However, under hydrogen deficient conditions, little conversion can be attributed to covalent bond rupture as indicated by a measured 20% conversion in naphthalene. 375°C should be sufficient to break most hydrogen bonds. Without a strong hydrogen bonding solvent, these bonds would reassociate as the liquefaction product cools to room temperature. With indole or another solvent capable of forming hydrogen bonds as strong or stronger than those present in the coal, these hydrogen bonding sites in the coal molecule are tied up as coal-indole bonds. Now as the product cools, reassociation between coal molecules does not occur and soluble coal-indole complexes are formed. This mechanism is shown in Figure 5. This type of mechanism is consistant with our data and suggest that a large fraction of the Wyodak "clusters" are held together solely by hydrogen bonds.

Conclusions

We have observed a high conversion of Wyodak coal to THF soluble products using indole as the liquefaction vehicle. We observed formation of hydrogen bonded complexes between indole and coal molecules. We determined that the important structural feature of indole is the N-H group which acts primarily as an electron-acceptor in forming hydrogen bonds. Solubilization of Wyodak coal in indole can best be represented by the pathway presented in Figure 5.

These results for Wyodak liquefaction in indole depict a liquefaction mechanism based on stabiliztion of hydrogen bonding sites in the coal. But more importantly, they indicate that a large fraction of Wyodak coal is crosslinked by hydrogen bonds. The large fraction of product which is produced as a complex with molecular weight near the classical asphaltene molecular weight range suggests that Wyodak coal is composed of clusters with molecular weights $\sim$160. This structural informaton suggests that a liquefaction procedure designed to attack the oxygen functionality responsible for hydrogen bonding in the coal would result in high conversion to a low molecular weight product.

Table 1. Proximate and Ultimate Analysis of Wyodak Coal (South Pit Mine)

Proximate*	
% Moisture	8.45
% Volatile	40.66
%Fixed Carbon	41.02
% Ash	9.87
	100.00

Ultimate*	
% Moisture	8.45
% Carbon	60.62
% Hydrogen	4.35
% Nitrogen	0.94
% Sulfur	0.68
% Oxygen (diff)	15.09
% Ash	9.87
	100.00

* Commercial Testing & Engineering Co., Denver, CO 80239

Table 2. Wyodak liquefaction results at 375°C, 20 minutes and 1000 psig nitrogen.

	Indole	Methylindole
	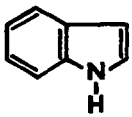	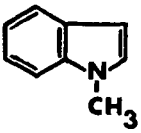
% THF Conversion	62%	35%

References

1. Tom Green, Jeffrey Kovac, Douglas Brenner, and John W. Larsen in "Coal Structure" (Ed., Robert A. Meyers), Academic Press, New York, 1982, pp. 199-282.

2. T. D. Padrick, M. G. Thomas and D. E. Trudell, presented at Gordon Conference on Fuel Science, Plymouth, NH, July 1981.

3. Dwain Spencer, EPRI Journal, May, p. 31 (1982).

4. John W. Larsen and Jeffrey Kovac in "Organic Chemistry of Coal" (Ed., John W. Larsen), American Chemical Society, Washington, DC, 1978, pp. 36-49.

5. Roman Pampuch, Prace Glownego Instytutu Goinictwa, No. 153, p. 1-16 (1954).

6. John W. Larsen, Yuda Yurum and Terry L. Sams, Fuel 62, 476 (1983).

7. John W. Larsen, Advanced Research & Technology Development Coal Liquefaction Projects Meeting, Pittsburgh, PA, October 1983.

8. Arthur W. Lynch and Michael G. Thomas, Fuel Processing Technology 8, 13 (1983).

9. D. C. Cronauer, R. D. McNeil and D. C. Young, Quarterly Progress Report for October-December 1981, DOE/PC/30080-7, June 1982.

Figure 1. Liquefaction results for Wyodak coal in quinoline type solvents.

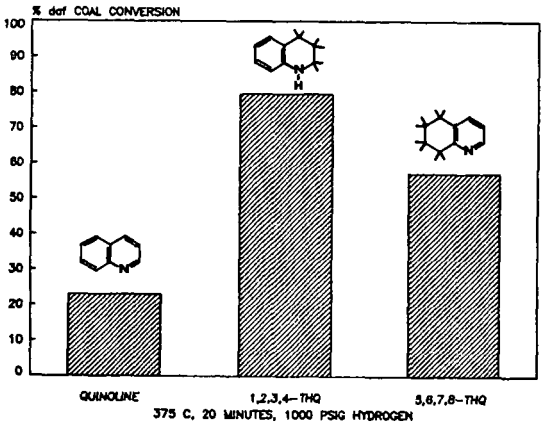

Figure 2. Liquefaction results for Wyodak coal in hydrogen donor solvents.

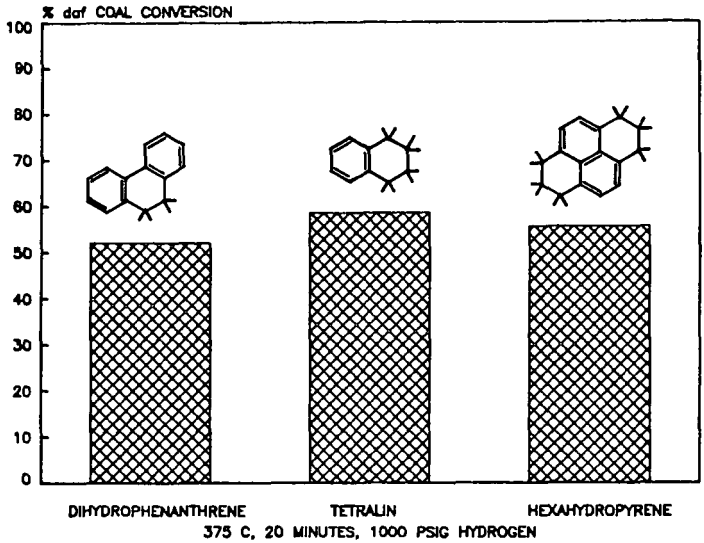

Figure 3. Liquefaction results for Wyodak coal in other basic solvents.

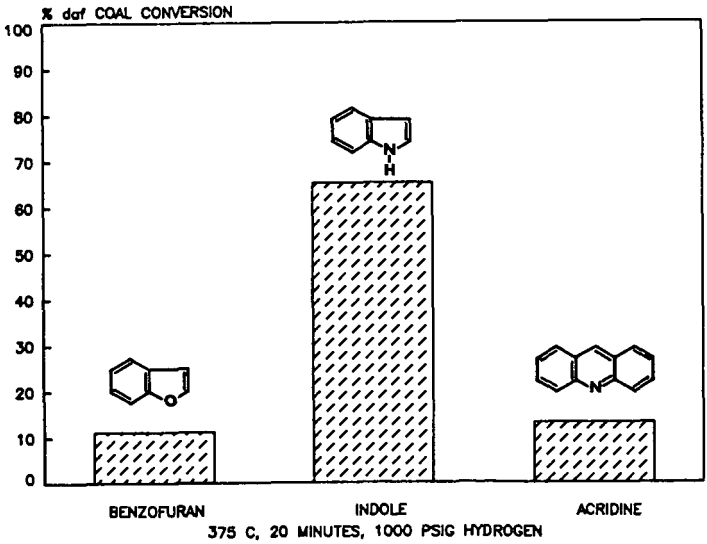

Figure 4. HPLC spectra of the THF soluble filtrate from microreactor runs.

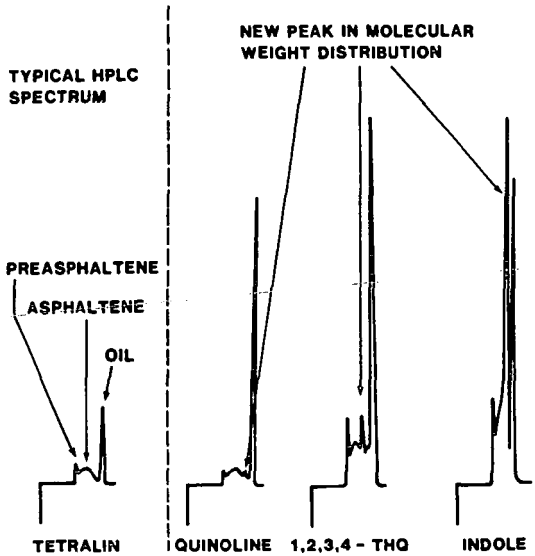

Figure 5. Indole disrupts hydrogen bonded coal matrix to form THF soluble complexes.

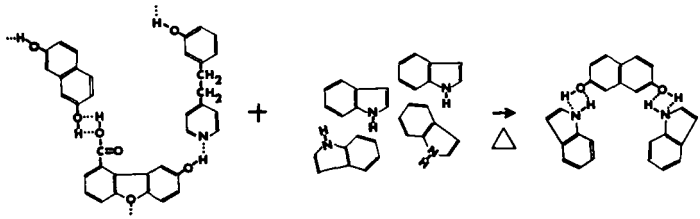

Hydrogen Bonded Coal + Indole → △ Hydrogen Bonded Complex

THERMAL REACTIVITY STUDIES OF SOLVENT REFINED COAL

R. L. Miller and N. Shankar
Chemical Engineering Department

University of Wyoming, Laramie, Wyoming 82071

ABSTRACT

Four solvent refined coal (SRC) samples obtained from Kentucky 9/14 and Illinois 6 coals have been thermally hydrogenated in a stirred microautoclave reactor at short contact time coal liquefaction reaction conditions. No coal or catalyst was used in any of the runs. Reactivity of each SRC sample was monitored using C_4-427°C distillate yield, hydrogen consumption, hydrogen-free gas make, and solvent solubility measurements.

Initial results indicated the existence of various interconversion reactions among the oil, asphaltene, preasphaltene, and pyridine insoluble organic matter (IOM) fractions of catalytically unhydrogenated Kentucky SRC at selected reaction conditions. The net result of this reaction sequence was a relatively high C_4-427°C distillate yield with minimal hydrogen-free gas make and hydrogen consumption. Kentucky and Illinois SRC samples which had been catalytically hydrogenated prior to use in the present study did not undergo the same types of reactions. Hydrogen-free gas make and hydrogen consumption were higher and C_4-427°C distillate yield was lower in runs using hydrogenated SRC samples.

INTRODUCTION

The primary reaction step in direct coal liquefaction is generally believed to involve thermal rupture of various labile bonds within the coal structure (1, 2, 3). If the reactive free radical coal fragments formed can be quickly capped with available hydrogen from a hydrogen-donor solvent or from portions of the coal itself (autostabilization), a complex mixture of stabilized products is obtained. For convenience, these mixtures have been operationally classified according to a series of solvent solubility tests summarized in Table I (4). Unfortunately, such a classification system does not produce fractions with simple chemical identities.

Preasphaltenes constitute the predominate primary liquefaction product with asphaltenes, oils (distillable and nondistillable), and gases formed in lesser amounts. Secondary reactions involving conversion of preasphaltenes and asphaltenes to produce additional quantities of oil and gas form an important part of coal conversion to distillable liquids. Furthermore, the use of residuum recycle has been shown to have a significant influence on liquefaction process performance. Silver reported that up to 50 wt% of the total distillate obtained in two-stage liquefaction of Wyodak coal could be attributed to conversion of mildly hydrogenated residuum (5). The need for a better understanding of residuum conversion to lighter products is necessary to further improve existing liquefaction processes.

The objective of the research described in this paper was to investigate the thermal conversion of coal-derived residuum in the absence of coal and catalyst at representative coal liquefaction conditions. Particular emphasis was placed on residuum behavior at short contact time reaction conditions similar to those employed in the Lummus ITSL process (6).

EXPERIMENTAL PROCEDURE

Solvent refined coal (SRC) produced from Kentucky 9/14 coal was used as feed residuum in the initial thermal reactivity experiments. This material, designated

F-51, boils above 427°C and was produced in the Pittsburg and Midway SRC-I pilot plant near Tacoma, Washington. To reduce SRC viscosity, blends of approximately 50 wt% F-51 and 50 wt% Kentucky 9/14 coal-derived distillate, designated F-7, were used as reactor feed. The F-7 distillate is a nominal 260-427°C boiling range fraction which was also produced at the Tacoma SRC-I pilot plant. Table II gives a brief description of F-51/F-7 properties.

Three other SRC-distillate mixtures were used in additional reactivity studies. Properties of these mixtures are also included in Table II. Sample F-102A was prepared by mildly hydrogenating a portion of F-51/F-7 at 370°C and 13.9 MPa initial cold hydrogen pressure for one hour over thermactivated Nalcomo 477 cobalt-molybdate catalyst in a batch reactor. Samples F-128 and F-129 are Illinois 6 coal-derived hydrotreated recycle residuum from Wilsonville, Alabama pilot plant runs 242 and 243, respectively. Run 242 was operated using a short contact time thermal reactor while run 243 utilized a long residence time dissolver. Both of these samples were obtained from essentially steady-state operations and represent residuum which had been recycled through the process many times. The C_4-427°C distillate content of both F-128 and F-129 was only about 30 wt%. Several reactivity runs were performed using F-128 or F-129 diluted with additional Illinois 6 coal-derived distillate to obtain feed mixtures containing about 50 wt% distillate. Results from these runs indicated that within experimental error, there was no effect on yields from the SRC when the feed distillate content was varied between 30 wt% and 50 wt%. Thus, yield data from the four SRC-distillate mixtures listed in Table II can be directly compared.

The thermal reactivity experiments were carried out in a 60 ml stirred microautoclave reactor system designed and constructed at the University of Wyoming. The reactor is similar to larger Autoclave batch reactors except that heating is accomplished with a high temperature sandbath. At the end of each run, the reactor and its contents are quenched with an icewater bath. This reactor system can provide the benefits of small tubing bomb reactors (quick heatup (~2 min.) and cool down (~30 sec.)) while at the same time insuring sufficient mechanical agitation of the reactants with an Autoclave Magnedrive II stirring assembly to minimize hydrogen mass transfer effects. Furthermore, the system is designed so that the reactor pressure is very nearly constant throughout an experiment.

The reactor runs were completed at 454°C and 6.9 MPa initial cold hydrogen pressure for reaction times in the range of 5 - 15 minutes. To simulate the slug flow behavior of commercial small diameter SCT reactors in which significant gas phase hydrogen mass transfer effects exist, the Magnedrive stirrer was turned off during these runs. These conditions are believed to simulate SCT operations reasonably closely.

Portions of the liquid products from each run were distilled to a 427°C endpoint using a microdistillation apparatus. Additional portions of the liquid product were sequentially extracted in a Soxhlet extractor using cyclohexane, toluene, and pyridine. Product gases were analyzed on an HP 5840A gas chromatograph.

RESULTS AND DISCUSSION

Using the experimental methods described, the product composition from each reactor run was measured. This data is summarized in Figures 1-4 in which weight fraction compositional changes as a function of reaction time are shown for each SRC-distillate sample. The weight fraction of hydrogen-free gas produced was always less than about 0.01 and is not shown on these figures. Results shown for F-51/F-7 are average values from duplicate runs, while data for the other three SRC-distillate samples were obtained in single runs. Based on previous experience with the reactor system and product analysis methods used, the weight fraction data presented has an experimental error of approximately ±10 relative percent.

Several interesting observations can be made from these results. First, a detailed examination of the material balance data indicates that the asphaltene fraction of F-51/F-7 formed both distillate and preasphaltenes particularly at reaction times greater than about 5 minutes. Several authors have previously noted this type of disproportionation behavior (7, 8, 9). In some cases these results have been interpreted as evidence of reaction "reversibility". However, as will be noted shortly, such reversibility does not really exist here, since the preasphaltenes formed by asphaltene disproportionation differ from the coal-derived preasphaltenes found in F-51/F-7. Figure 1 also shows a decline in the nondistillable oil content most likely caused by thermal cracking of oils to form additional distillate and gas. No significant amount of pyridine insoluble organic matter (IOM) was formed during the F-51/F-7 runs.

In contrast, results shown in Figures 2-4 for the hydrogenated SRC-distillate samples indicate somewhat different behavior. In each case, the asphaltene fraction apparently shows no propensity toward disproportionation. Rather, material balance data suggests that preasphaltenes and asphaltenes were slowly converted to nondistillable oils, and eventually cracked to distillate and gas in a series type mechanism. After about ten minutes reaction time, the conversion of nondistillable oils to distillate and gas was the only significant reaction taking place in the F-128 and F-129 samples. Once again, very little IOM was produced in any of the runs. This is not surprising since other researchers have noted the refractory nature of hydrogenated asphaltenes toward thermal or catalytic conversion to lower boiling products (10, 11).

The overall effect of differences in asphaltene and preasphaltene thermal reactivity between the unhydrogenated and hydrogenated SRC-distillate samples is summarized in Figure 5. In this plot, hydrogen utilization efficiency defined as the mass of C_4-427°C distillate produced per unit mass of hydrogen consumed is plotted as a function of reaction time for each of the four SRC-distillate samples. The unhydrogenated F-51/F-7 sample obviously produces a significant amount of distillate with minimal hydrogen consumption when compared with yield data from the hydrogenated samples. Furthermore, Figure 6 shows that the hydrogen-free gas make was found to be 2 to 6 times less in the F-51/F-7 runs. It appears that asphaltene disproportionation is a more efficient method of distillate production than thermal cracking of nondistillable oils. However, it is apparent that even mild catalytic hydrotreatment of the SRC results in drastically reduced hydrogen utilization efficiency.

In an attempt to further study differences between the reaction pathways of unhydrogenated and hydrogenated asphaltenes and preasphaltenes, the preasphaltene fractions from the F-51/F-7 and F-102A thermal reactivity experiments were subdivided into chloroform soluble-toluene insoluble and pyridine soluble-chloroform insoluble subfractions, designated preasphaltene-1 and preasphaltene-2, respectively. Boduszynski has reported that preasphaltene-1 samples generally resemble asphaltenes in the number of function groups and degree of aromaticity (12). Preasphaltene-2 samples are more highly functional and are believed to fairly well represent coal-derived preasphaltene material. As shown in Figure 7, the increase in total preasphaltene content for the F-51/F-7 runs was due to an increase in preasphaltenes-1. At least a portion of the preasphaltenes-1 was obtained as a disproportionation product from the asphaltenes. The fact that the total preasphaltene content did not remain constant or decrease precludes the reaction sequence: preasphaltenes-2 to preasphaltenes-1 to asphaltenes as the only pathway involving these fractions. In contrast, as shown in Figure 8, the decrease in F-102A preasphaltenes occurred because of preasphaltenes-2 consumption. No significant buildup of preasphaltenes-1 was noted. Once again, this suggest that F-102A asphaltenes did not undergo disproportionation.

The exact mechanism responsible for the apparent change in asphaltene reactivity is not yet known. Painter (13) and Whitehurst (14) have indicated that retrogressive reactions of SRC fractions to ultimately form char involve the condensation of alkyl and phenolic functional groups rather than direct aromatic ring fusing. It is quite possible that the same functional groups are involved during asphaltene disproportionation. Catalytic hydrotreatment of the SRC would result in fewer available functional groups with which the disproportionation could occur. Efforts are currently underway to test this hypothesis by observing detailed structural changes of the F-51/F-7 and F-102A preasphaltene and asphaltene fractions during thermal hydrogenation.

CONCLUSIONS

The thermal reactivity behavior of one unhydrogenated and three hydrogenated SRC-distillate samples has been studied at simulated short contact time (SCT) reaction conditions. Unhydrogenated coal-derived asphaltenes were found to disproportionate into primarily C_4-427°C distillate and preasphaltene-1 material resulting in high hydrogen utilization efficiency and low hydrogen-free gas make. Asphaltenes from the hydrogenated SRC-distillate samples did not disproportionate. As a result, hydrogen utilization efficiency was significantly lower and hydrogen-free gas make was higher in runs using the hydrogenated samples.

ACKNOWLEDGEMENTS

Financial support for this research was provided by the Electric Power Research Institute under Contract Number RP 1604-04. Mr. Norman Stewart of EPRI provided helpful comments.

LITERATURE CITED

1. Farcasiu, M., ACS Div. Fuel Chem. Preprints, 24, 1, 121, (1979).

2. Han, K.W., and Wen, C.Y., Fuel, 58, 779, (1979).

3. Neavel, R.C., Fuel, 55, 237, (1976).

4. Schweighardt, F.K., Retcofsky, H.L., and Raymond, R., ACS Div. Fuel Chem. Preprints, 21, 7, 27, (1976).

5. Silver, H.F., Corry, R.G., Miller, R.L., and Hurtubise, R.J., Fuel, 61, 111, (1982).

6. Schindler, H.D., Chen, J.M., and Peluso, M., "Liquefaction of Eastern Bituminous Coals by the Integrated Two-Stage Liquefaction (ITSL) Process", Proceedings of the Seventh Annual EPRI Contractors' Conference on Coal Liquefaction, Palo Alto, California, (May, 1982).

7. Thomas, M.G., "Catalyst Behavior in Direct Coal Liquefaction", Proceedings of the Sixth Annual EPRI Contractors' Conference on Coal Liquefaction, Palo Alto, California, (May, 1981).

8. Lee, W.C., Interconversion of Coal-Derived Products, Ph.D. Dissertation, University of Southern California, (1980).

9. Farcasiu, M., Mitchell, T.O., and Whitehurst, D.D., ACS Div. Fuel Chem. Preprints, 21, 7, 11, (1976).

10. Baldwin, R.M., Personal Cummunication, (1983).

11. Silver, H.F., Corry, R.G., and Miller, R.L., "Coal Liquefaction Studies", Final Report for EPRI Projects 779-23 and 2210-1, (December, 1982).

12. Boduszynski, M.M., Hurtubise, R.J., and Silver, H.F., Anal. Chem., 54, 375, (1982).

13. Painter, P.C., Yamada, Y., Jenkins, R.G., Coleman, M.M., and Walker, P.L., Jr., Fuel, 58, 4, 293, (1979).

14. Whitehurst, D.D., Mitchell, T.O., Farcasiu, M., and Dickert, J.J., Jr., "The Nature and Origin of Asphaltenes in Processed Coal", Final Report for EPRI Project 410, vol. 2, (December, 1979).

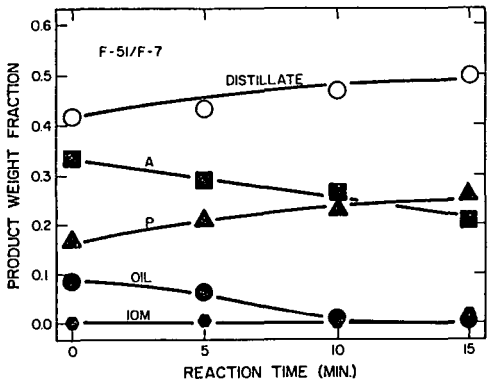

Figure 1 - Product Distribution for F-51/F-7 Runs

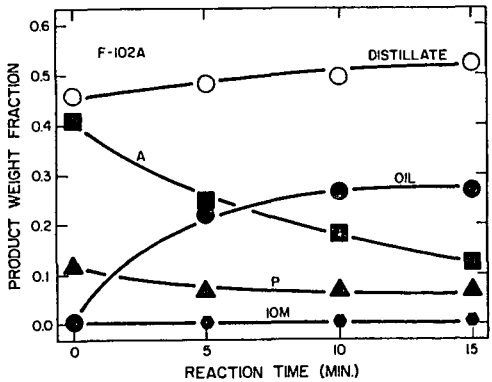

Figure 2 - Product Distribution for F-102A Runs

Table I

Classification of Coal Liquefaction Products

Fraction	Definition
Insoluble Organic Matter	Pyridine or THF insoluble
Preasphaltenes	Pyridine or THF soluble; benzene or toluene insoluble
Asphaltenes	Benzene or toluene soluble; pentane, hexane, or cyclohexane insoluble
Oils	Pentane, hexane, or cyclohexane soluble

Table II

SRC - Distillate Feed Mixture Properties

SAMPLE	F-51/F-7	F-102A	F-128	F-129
SOURCE COAL	KY 9/14	KY 9/14	ILLINOIS 6	ILLINOIS 6
WT.% BOILING ABOVE 427°C	58.0	54.8	68.5	69.2
HYDROGENATION LEVEL	NONE	MILD	SEVERE	SEVERE
ULTIMATE ANALYSIS (WT% DRY BASIS)				
CARBON	86.4	86.9	89.1	89.3
HYDROGEN	7.1	8.0	8.9	8.9
NITROGEN	1.9	1.5	0.4	0.6
SULFUR	0.8	0.6	0.1	0.1
OXYGEN (DIFFERENCE)	3.7	2.9	1.1	0.9
ASH	0.1	0.1	0.4	0.2

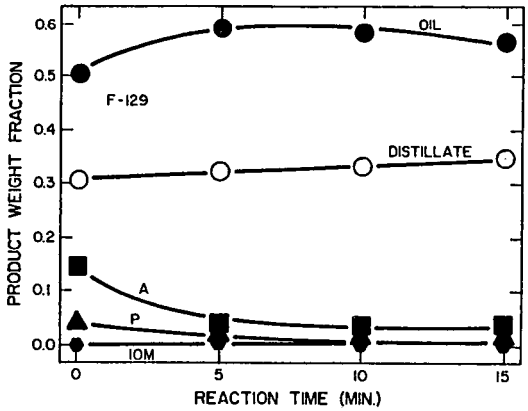

Figure 4 - Product Distribution for F-129 Runs

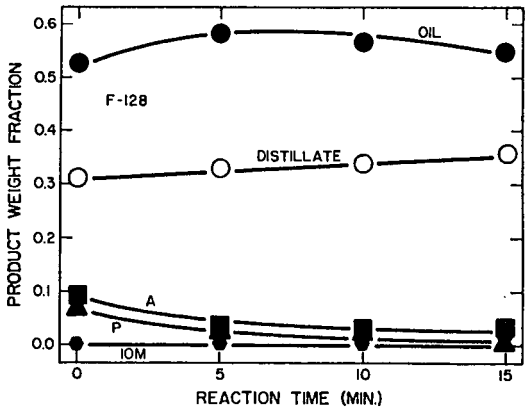

Figure 3 - Product Distribution for F-128 Runs

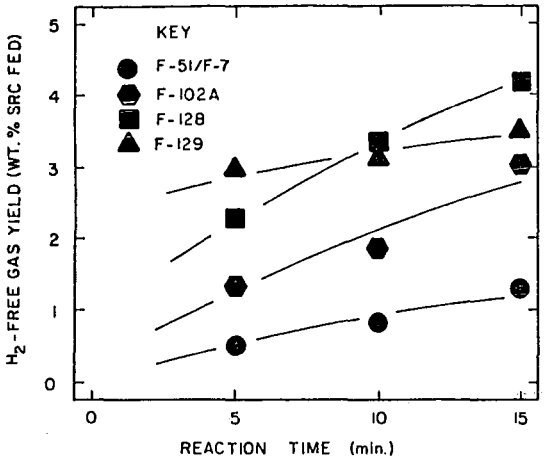

Figure 6 - Hydrogen-free Gas Yield as a Function of SRC Feedstock and Reaction Time

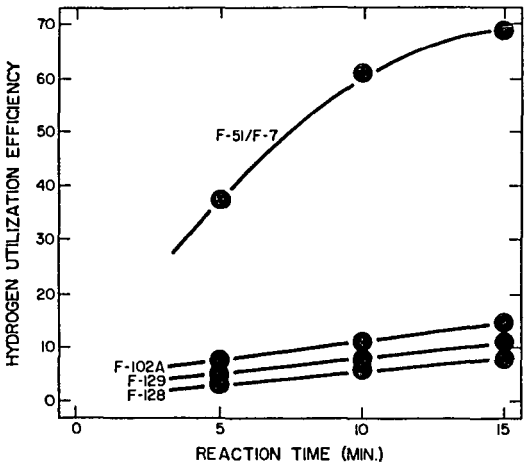

Figure 5 - Hydrogen Utilization Efficiency as a Function of SRC Feedstock and Reaction Time

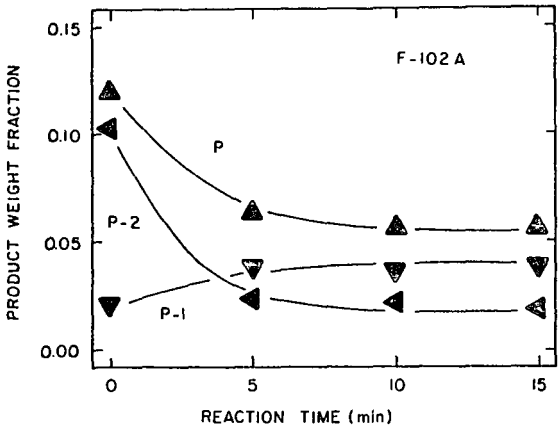

Figure 8 - Preasphaltene Composition for F-102A Runs

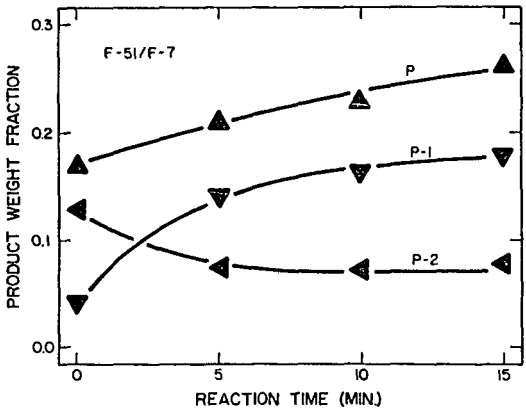

Figure 7 - Preasphaltene Composition for F-51/F-7 Runs

ANALYSIS OF RESINS IN HIGH-ASH COAL-DERIVED PRODUCTS

F. M. Lancas, H. S. Karam and H. M. McNair
Department of Chemistry
Virginia Polytechnic Institute and State University
Blacksburg, VA 24061

INTRODUCTION

The past few years have witnessed extensive efforts to characterize coal-derived liquids. One widely used method to characterize these liquids is the SARA fractionation method by which the fossil fuel is fractionated into saturates, aromatics, resins and asphaltenes. One of these fractions, resins, is believed to play an important role in the conversion process of coal into liquid products. Liquid chromatography and solubility tests are two different approaches to the SARA fractionation. Following precipitation of asphaltenes in non-polar hydrocarbons (such as n-pentane), the deasphaltened solution can be chromatographed on silica or alumina to obtain the resins. The deasphaltened solution can also be applied to a clay column and eluted with pentane to separate resins from oils, or it can be treated with propane gas to precipitate the resins.

In this paper, resins obtained by five different methods are compared gravimetrically and by reverse phase high performance liquid chromatography. These methods are: 1) the Phillips Petroleum procedure; 2) our alternative SARA procedure; 3) fractionation by solubility; 4) fractionation by clay; and 5) our new preparative scale LC method.

Experimental

a) Preparation of resins by the different methods

The five methods investigated are conducted on the same coal, a high ash Brazilian "Mina Do Leao" coal, under the same conditions of sample preparation, extraction, and solvent evaporation. Such experimental conditions are described in detail in our previous work (1).

The Phillips Petroleum Procedure: Method 1

Ten gm coal, 60 mesh, are extracted with 100 ml hexane and the insolubles (asphaltenes) are filtered through a Whatman No. 1 cellulose filter paper. A portion of the hexane extract is applied to the top of a glass column (500 x 11 mm) dry packed with 20 gm alumina, activity I, 80-200 mesh (Fisher Scientic, Pittsburg, PA). Saturates are eluted with 50 ml of hexane; aromatics with 75 ml of touene; and resins with 50 ml of methanol (1,2).

The Alternative SARA Method: Method 2

This is an improved method developed in our laboratory at VPI (1). Coal is extracted with tetrahydrofuran (THF) and the unreacted coal is removed by filtration. The coal derived product, after removal of the solvent, is dissolved in 1 ml THF; then it is applied to the top of a glass column (500 x 11 mm) slurry packed with 20 gm of silica gel 60 - 200 mesh (Fisher Scientific, Pittsburg, PA). Saturates are eluted with 50 ml of hexane; aromatics with 75 ml of toluene; resins with 50 ml of methanol; and asphaltenes with 50 ml of THF.

Fractionation by Solubility: Method 3

Following extraction of the coal with tetrahydrofuran (THF) and removal of the solvent; the coal-derived product is dissolved in 2 ml of THF then treated with 80 ml of n-pentane to precipitate the asphaltenes (3). The volume of the deasphaltened solution (maltenes) is reduced to 30 ml by evaporation, then placed in an ice-water bath and an excess of propane gas (99% chemically pure) is added with constant stirring, thus precipitating the resins (3). The solution is then filtered through a Whatman No. 1 cellulose filter, and the precipitate washed with propane-saturated pentane, dried, then weighed.

Fractionation by Attapulgus (florsil) column: Method 4

The deasphaltened solution, as obtained in method 3, is stripped off solvent then dissolved in 1 ml of a 1:1 mixture acetone:methylene chloride. This solution of maltenes is applied to the top of a glass column (500 x 11 mm) slurry packed with 12 gm florisil, 60-100 mesh (Supelco, Bellefonte, PA). Seventy-five ml n-pentane are passed to elute "the oils", while 50 ml of 1:1 acetone:methylene chloride are passed afterwards to elute the retained "resins" in accordance with the literature (4).

New Preparative Scale LC Fractionation: Method 5

Following extraction and solvent evaporation, the THF coal derived product is dissolved in 1 ml THF, then applied to the top of a glass column (500 x 11 mm), slurry packed with 20 gm silica gel, 40-60 mesh Si-60 (EM Science, Gibbstown, NJ). Eight fractions are collected from the preparative scale column in the following order: saturates, monoaromatics, diaromatics, triaromatics, polynuclear aromatics, resins, asphaltenes and and asphaltols. Table 1 shows the eluents utilized to give the best separation among the group types; the volumes used; and the fractions eluted. More details about this method can be found in the literature (5). Figures 1 and 2 show the chromatograms obtained for the non-polar and polar fractions.

TABLE 1

Eluents and Fractions Collected in the Preparative Scale Fractionation Method: Method 5

Fraction Eluted	Eluent	Volume (ml)
1. Saturates	Hexane (C_6)	40
2. Monoaromatics	Hexane (C_6)	27
3. Diaromatics	11.5% benzene in C_6	36
4. Triaromatics	32.0% benzene in C_6	24
5. Polynuclear aromatics	32.0% benzene in C_6	25
6. Resins	Benzene/$(CH_3)_2CO$/$MeCl_2$(3/4/3)	65
7. Asphaltenes	$(CH_3)_2CO$/THF(2/8)	60
8. Asphaltols	Pyridine	65

b) High Performance Liquid Chromatographic Separation

The analytical instrument used was a Varian Model 5020 High Performance Liquid Chromatograph. Detection was made using a Varian Varichrom Detector at 254 nm. The peaks were recorded on a Varian Model 9176 recorder. A high pressure sixport Valco valve model N-60 was utilized with a sample loop of 10 µl. The column used was 150 x 4 mm Micropak 5µ, RP-18. Mobile phase was a 70/30 acetonitrile/water at a flow rate of 1 ml/min. Each resins fraction, after removal of the solvent, was dissolved in THF to a concentration of 10 mg/ml. The solutions were then double filtered through 5.0 µm Millipore filters (type LS) and finally diluted to a concentration of 0.4 mg/ml with acetonitrile prior to injection on the HPLC system.

Results and Discussion

a) Gravimetric analysis of resins

Table 2 displays a comparison of the relative distribution of resins among the five methods investigated as applied to the Brazilian coal.

TABLE 2

Relative Distribution of Resins in the Brazilian Coal Extract Using Different Separation Methods

Method	Wt. % Resins*	σ	% σ (RSD)
1. Phillips	29.4	10	35
2. Alternative SARA	51.8	---	---
3. Fractionation by solubility	15.1	0.44	2.9
4. Fractionation by Clay	10.5	0.15	1.4
5. LC Preparative Scale	57.8	0.33	0.57

*Results from 4 repetitive runs

Table 2 shows that method 5 is by far the most reproducible system investigated. In both methods 2 and 5, resins are the major fraction in the coal-derived product. It is important to note that in methods 2 and 5 the whole THF coal extract was applied to the chromatographic column without any previous precipitation of asphaltenes (methods 1, 3, 4) or resins (method 3). The new preparative scale LC method is more complete than method 2, yielding eight discrete and pure chemical classes as has been evidenced by HPLC (see figures 1 and 2). In addition, it has a recovery of more than 94% of the loaded sample (6). The fractionation of the whole coal extract by this method yields purer fractions than those obtained by the traditional solubility fractionation, thus avoiding the contamination by co-precipitation commonly encountered in this method (1). In a different set of experiments, an asphaltenes sample (benzene soluble, pentane insoluble) from the solubility fractionation method was studied by the new method and the result showed that what seemed to be asphaltenes was in fact more than 70% resins (7).

High Performance Liquid Chromatography Analysis

The chromatogram in figure 3 is for a standard mixture of polar compounds found in coal-derived liquids. A range of functional groups was chosen to represent many of the compound classes which could be found in coal. Structures of these compounds are shown in figure 3. Figure 4 shows a chromatogram for resins produced by method 5 while figures 5 and 6 show chromatograms for resins produced by methods 4 and 3. It is important to note that all resin solutions were chromatographed under identical conditions. Figure 3 shows that the column is very efficient. Figures 4, 5 and 6 show that the resin fraction obtained from coal by several separation procedures is still extremely complex and even better sample separation schemes need to be developed. We are continuing efforts along these lines.

Conclusion

Both gravimetric and HPLC results show that depending on the fractionation method of the coal-derived product one gets different distributions of resins. Among the different methods studied, the new preparative LC scale method seems to yield purer fractions; it produces a higher yield of sample (94%); and it is a complete method that fractionates the whole coal derived product in a single step without the inconvenience of precipitating asphaltenes or resins.

REFERENCES

1. Lancas, F. M., Karam, H. S. and McNair, H. M. Preprint Am. Chem. Soc., Div. Fuel Chem., Vol. 28, No. 4, 1983

2. Phillips Petroleum Company, Research and Development Method 8045-AS(1980)

3. Bunger, J. W., and Li, N. C., eds., "Chemistry of Asphaltenes; advances in Chem. Series." No. 195, AMS (1981)

4. Galya, L. G. and Suatoni, J. C. J. Liquid Chrom. 3,229-242(1980)

5. Lancas, F. M., Karam, H. S. and McNair, H. M. Paper submitted to J. Chromatography, Oct. 1983

6. Lancas, F. M., Karam, H. S. and McNair, H. M., in preparation

7. Karam, H. S. Unpublished results

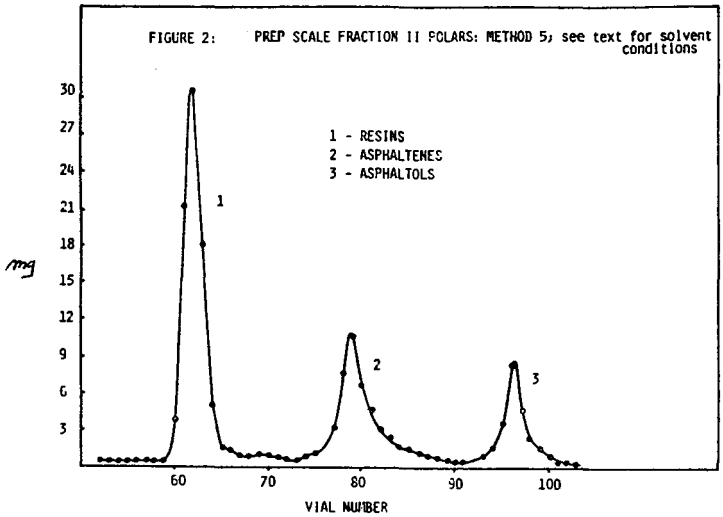
FIGURE 2: PREP SCALE FRACTION II POLARS: METHOD 5; see text for solvent conditions
1 - RESINS
2 - ASPHALTENES
3 - ASPHALTOLS
mg
30
27
24
21
18
15
12
9
6
3
1
2
3
60
70
80
90
100
VIAL NUMBER

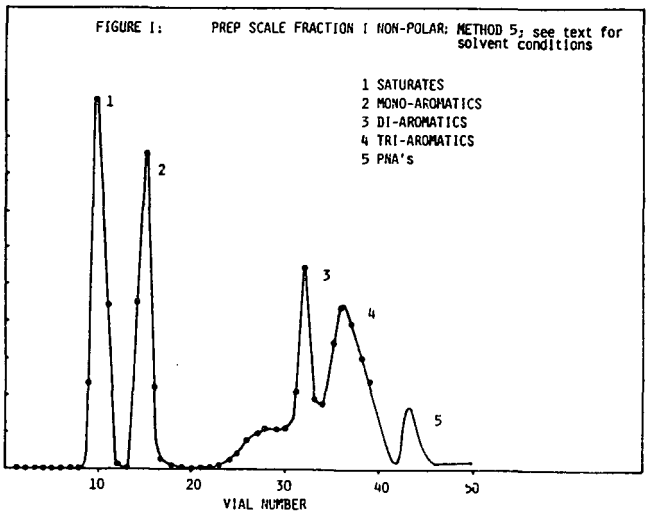
FIGURE I: PREP SCALE FRACTION I NON-POLAR: METHOD 5; see text for solvent conditions
1 SATURATES
2 MONO-AROMATICS
3 DI-AROMATICS
4 TRI-AROMATICS
5 PNA's
1
2
3
4
5
10
20
30
40
50
VIAL NUMBER

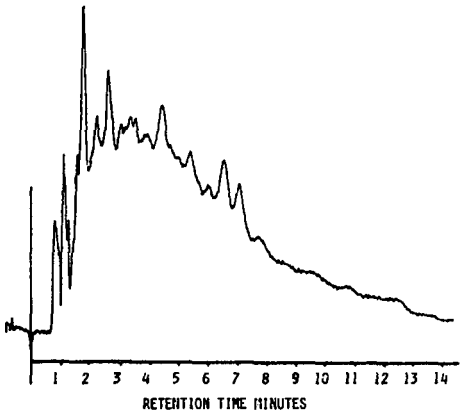

FIGURE 4: RESINS FRACTION PRODUCED BY METHOD 5
ISOCRATIC; 70/30 ACETONITRILE/WATER
2 ml/min. U.V. AT 254 x 0.05 AUFS

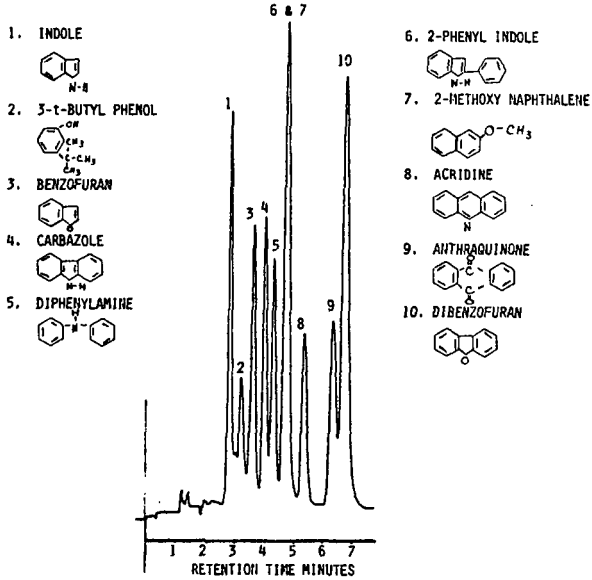

FIGURE 3: REVERSE PHASE SEPARATION OF
STANDARD MIXTURE; TEMPERATURE AMBIENT:
COLUMN 150 x 4 mm RP-18 MICROPAK 5μ,
FLOW RATE 1ml/min ISOCRATIC: 70/30
ACETONITRIL/WATER U.V. AT 254 nm,
0.2 AUFS

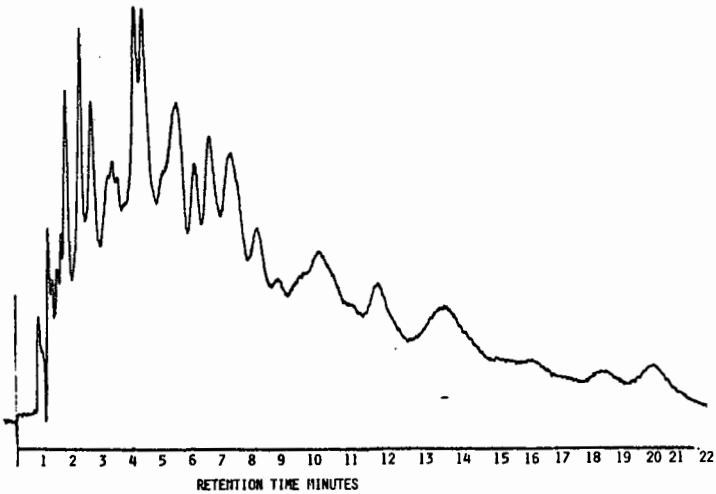

FIGURE 6: RESINS FRACTION PRODUCED BY METHOD 3; conditions same as figure 4

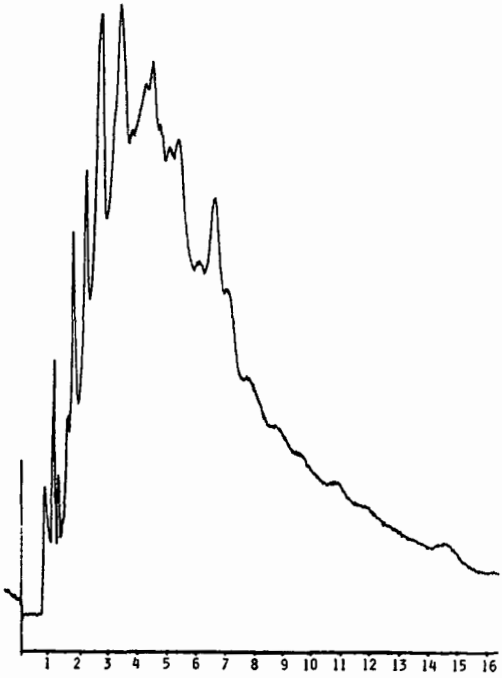

FIGURE 5: RESINS FRACTION PRODUCED BY METHOD 4; conditions same as figure 4

Oxygen Absorption and Light Scattering Studies of the Stability of Liquid Fuels

by N.F. Yaggi,[1] S.H. Lee,[1] J. Ge[1] and N.C. Li[1, 2]

[1]Duquesne University, Department of Chemistry, Pittsburgh, PA 15282 and

[2]Department of Chemistry, Catholic University of America, Washington, D.C. 20064

INTRODUCTION

Extensive literature (1, 2) have shown that 2,5-dimethylpyrrole (DMP) is particularly deleterious to stability of liquid fuels, in that this alkylated pyrrole promotes very drastically the formation of insoluble sediments and adherent gums. DMP also promotes extensive light scattering and oxygen absorption, so that their measurements are useful in monitoring the instability of liquid fuels. When the methyl group is on the ring nitrogen in pyrrole, as in N-methyl pyrrole (NMP), the ability to promote sediment formation, light scattering and oxygen absorption becomes much less.

Smith and Jensen (3) have given data on consumption of oxygen by pure pyrroles and have shown that at 323K, the oxygen uptake by DMP is much higher and faster than NMP. The purpose of this research is to determine whether results of oxygen absorption, light scattering and deposit formation can be correlated in studying the instability of liquid fuels. The liquid fuels used are SRC-II and H-coal middle distillates and the upgraded liquids prepared by Chevron Research Co. (4), as well as petroleum-derived JP-5 fuels. Synergistic effects between DMP and thiophenol have been found and are reported in this paper also.

EXPERIMENTAL

The apparatus used for determination of oxygen absorption is shown in Figure 1. It is a semi-closed atmospheric pressure unit in which a static atmosphere of oxygen over an aqueous manometric fluid (Krebs' manometer fluid (5)) is allowed to come in contact with a vigorously stirred sample for ageing. The loss of volatile material during ageing is minimized by the use of an efficient water condenser and a cold trap connected in tandem. In a typical experiment the side-arm flask containing a weighed sample is attached to the bottom of the water condenser. With all the stopcocks open and the reservoir R filled with Krebs' manometer fluid, oxygen gas is passed through the entire system for several seconds. Then the side-arm stopcock is closed and the reservoir is filled with oxygen to a point between the 425 and 450 ml marks. The oxygen inlet stopcock A is then closed and the leveling bulb B is adjusted so as to maintain the same liquid levels in R and B. One or more initial readings of atmospheric pressure, ambient temperature and gas volume in R are made. Additional readings are made, usually 3-5 times a day, for several days, until the liquid level in R neared the "0 ml" mark or the oxygen uptake appeared to stop.

Laser light scattering measurements were carried out with a photometer described by Berry (6) modified by introduction of a laser light source (Spectra-Physics Model 155 0.5 mW He-Ne laser, 632.8 nm). Light scattering cells of the design by Dandliker and Kraut (7) were used. The Pyrex cells were in the form of truncated cones, in order to reduce the stray light pickup by the detector. The additives were weighed in volumetric flasks and then filled to the mark with liquid fuel; the time of mixing was taken as zero time. The liquid was then introduced into a light-scattering cell; the cell was mounted on a cell holder, which in turn was mounted in a cell compartment. Care was taken to insure proper alignment of the cell with the very narrow light beam and the detector. The instrument was calibrated periodically by replacing the cell with a turbid standard glass block. The experiments were conducted at 298 ± 2K.

SRC-II process products were made from Pittsburgh Seam Coal at Pittsburg and Midway Coal Co. These products were blended in the ratio recommended by the Department of Energy Technical officer to represent a typical net whole liquid product from the SRC-II process. The blend is referred to as SRC-II syncrude. H-coal process products derived from Illinois no. 6 coal were blended in the ratio recommended by Hydrocarbon Research Inc. to represent a net whole liquid product from the H-coal process. This blend is referred to as H-coal syncrude. The syncrudes (or middle distillates) were hydrotreated using Chevron's ICR catalyst (containing nickel, tungsten, silica and alumina) at 672 K and approximately 15.6 MPa H_2 partial pressure. The properties of the syncrudes and their upgraded liquids are listed in Table 1 of ref. (4). Petroleum-derived JP-5, no. 80-8 and no. 80-12, were obtained from the Naval Research Laboratory.

RESULTS AND DISCUSSION

Figure 2 shows oxygen uptake curves obtained at 323 K for a middle distillate, an upgraded coal liquid, and petroleum JP-5. The coal-derived middle distillate shows much higher oxygen uptake than the upgraded liquid, which in turn is only slightly greater than the petroleum jet fuel. This means that Chevron Research Inc. have upgraded the coal liquid to about the same stability characteristics (as shown by the extent of oxygen uptake) as the petroleum jet fuel. Other characteristics of the upgraded coal liquids have been discussed in ref. (4).

Figure 3 shows oxygen uptake of SRC-II syncrude at 348 K in the absence and presence of 0.1 g copper shavings per 5 g of fuel. Several investigators (8-10) have discussed copper catalysis of the ageing of SRC-II middle distillate by a phenol oxidative coupling mechanism, and Figure 3 shows that the copper catalysis is also manifested by increase in oxygen uptake.

IR spectra of dilute solutions of SRC-II middle distillate (from Illinois no. 6 coal), before and after ageing for 5 days at 335 K, have been published by Jones and Li (9). The unaged coal liquid exhibits a prominent free hydroxyl stretching band at 3600 cm^{-1}. The intensity of this band is not significantly affected by ageing with copper or oxygen alone; but with both the intensity of this band is reduced. This indicates that the hydroxyl group is modified during ageing, and that the presence of copper is necessary. The unaged coal liquid is completely soluble in pentane. However, after ageing for 5 days with Cu + O_2 at 335 K, 30% of the aged coal liquid became insoluble in pentane. The insoluble fraction contained 3.5% copper in oxidation state II (10). The fact that copper (II) is present signifies that it acts as a reactant in addition to its role as a catalyst.

Iron (II) phthalocyanine (PcFe) also acts as a catalyst in the oxygen uptake by H-coal middle distillate, as shown in Figure 4. In the absence of PcFe, a long induction period of 160 hrs. exists. In the presence of 0.025 g PcFe in 5 g of the middle distillate, the induction period disappears, and a significant oxygen uptake occurs. This constitutes an example of the use of PcFe as a catalyst in the oxidation of coal liquids. Kropf (11) has previously proposed that, in the oxidation of cumeme below 373 K, copper phthalocyanine activated a molecular oxygen through its coordination with the metal ion to form a phthalocyanine-O_2 complex, which then abstracted the tertiary hydrogen of cumeme to initiate the oxidation. Hara et al. (12) found that the addition of a small amount of pyridine to metal-Pc and cumene mixtures induced a drastic shortening of the induction period and a considerable increase in oxidation rate. In our experiment (Figure 4) addition of pyridine is not necessary, since the H-coal middle distillate already contains many nitrogen-containing compounds.

Figure 5 gives plots of moles O_2 absorbed per mole of N-methyl pyrrole (NMP) vs. time at three temperatures. Increase in temperature means increase in accelerated ageing and therefore results in greater oxygen uptake. At a given temperature, longer storage time results in more ageing and greater oxygen uptake. Jones, Hardy, and Hazlett (13) have shown that for petroleum-derived diesel fuel marine, increase in stress temperature results in a shorter time necessary to form equivalent weights of total insolubles. The data of Fig. 5 also show that increase in temperature results in a shorter time necessary to absorb equivalent amount of oxygen per mole of NMP. A plot of log t vs. 1/T can be constructed, where t is the time in hours required at any particular temperature of stressing to absorb 0.01 mole O_2/mole NMP. The plot is almost linear. Figure 5 also shows that 2,5-dimethylpyrrole (DMP) exhibits much higher oxygen uptake than does NMP. This is in line with the fact (1, 2) that DMP promotes very drastically the formation of insoluble gums and light scattering in fuels, whereas the effect of NMP is very small. Reactions leading to sediment formation may be characterized as free radical, autoxidative reactions. The greater extent of radical formation in DMP may explain in part the greater oxygen uptake by DMP than NMP and the greater ability to promote deposit formation and light scattering, by DMP than by NMP.

Figure 6 shows plots of light scattering intensity at 90° scattering angle for petroleum JP-5 containing 50 ppm (N) DMP and various additives. The presence of 0.2M thiophene, 0.2 M 1,5-hexadiene, or 0.2M thiophenol alone in the petroleum JP-5 results in no change in I_{90}. In the presence of DMP however, thiophenol gives the largest light scattering followed by hexadiene and then thiophene. The implication is that these individual sulfur-containing compounds by themselves are not deleterious to the stability of the liquid fuel. However, in the presence of nitrogen-containing compound like DMP, the instability effect is shown. Therefore, the combined effect of nitrogen and sulfur-containing compounds must be considered. Figure 7 shows similar plots for upgraded H-coal. Here the scattering angle is 45°, because the intensity at 90° is too small to differentiate between the different additives. The order of instability is: thiophenol $>$ 1, 5-hexadiene $>$ 1-hexene, $>$ thiophene.

Figure 8 gives plot of I_{90} vs. time for 2, 6-dimethylquinoline (DMQ) and additives vs. time.

In our experiments, positive synergism involving DMP or DMQ is greatest for thiophenol, and the order of other sulfur compounds and unsaturated compound, is the same, whether the fuel is petroleum, upgraded H-coal or upgraded SRC-II liquids. DMQ has less effect on light scattering than DMP, and promotes much less deposit formation than DMP.

CONCLUSIONS

Coal-derived middle distillates have higher oxygen uptake than upgraded coal liquids, which in turn are only slightly higher than the petroleum jet fuel. DMP promotes oxygen absorption, light scattering, and deposit formation, much more than NMP. These three techniques can be correlated in studying the instability of liquid fuels. Synergistic effects between nitrogen and sulfur-containing compounds are apparent.

ACKNOWLEDGEMENT

The support of the U.S. Department of Energy to Duquesne University and the Naval Air Systems Command to Catholic University of America is acknowledged. Thanks are due to G. Berry for use of the light scattering facility at Carnegie-Mellon University, R. Sullivan for generously supplying the upgraded coal liquids, and R.N. Hazlett for helpful discussions.

REFERENCES

(1) Brinkman, D.W., Frankenfeld, J.W., Taylor, W.F. and Bruncati, R.L., Fundamental Synthetic Fuel Stability Study, DOE/BC/10045-23, 1982; other DOE reports

(2) Jones, L., Hazlett, R.N., Li, N.C., and Ge, J., ACS Div. Fuel, Chem. Preprints, 28 (1), 196 (1983)

(3) Smith, E.B. and Jensen, H.B., J. Org. Chem., 1967, 32, 3330

(4) Young, L-J.S., Li, N.C., Hardy, D., Fuel, 1983, 62, 718

(5) Krebs, H.A., Biochem. J., 1951, 48, 240

(6) Berry, G.C., J. Chem. Phys. 1966, 44, 4550

(7) Dandliker, W.B. and Kraut, K.F. J. Am. Chem. Soc. 1956, 78, 2380

(8) Hara, T., Jones, L., Li, N.C., and Tewari, K.C., Fuel 1981, 60, 1143

(9) Jones, L. and Li, N.C. Fuel, 1983, 62, 1156

(10) White, C.M., Jones, L., and Li, N.C. Fuel, in press

(11) Kropf, H. Ann. Chem.1960, 637, 73

(12) Hara, T., Ohkatsu, Y. and Osa, T. Bull. Chem. Soc. Japan, 1974, 48, 85

(13) Jones, L., Hardy, D., and Hazlett, R.N. Preprint, ACS Div. Petrol. Chem., 1983, 28(5), 1157

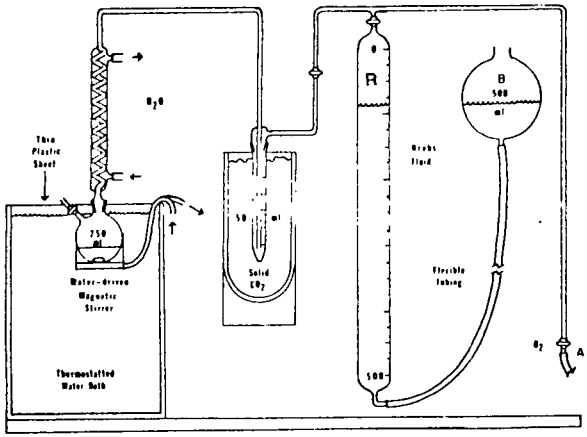

Fig. 1 Apparatus for oxygen-consumption measurement

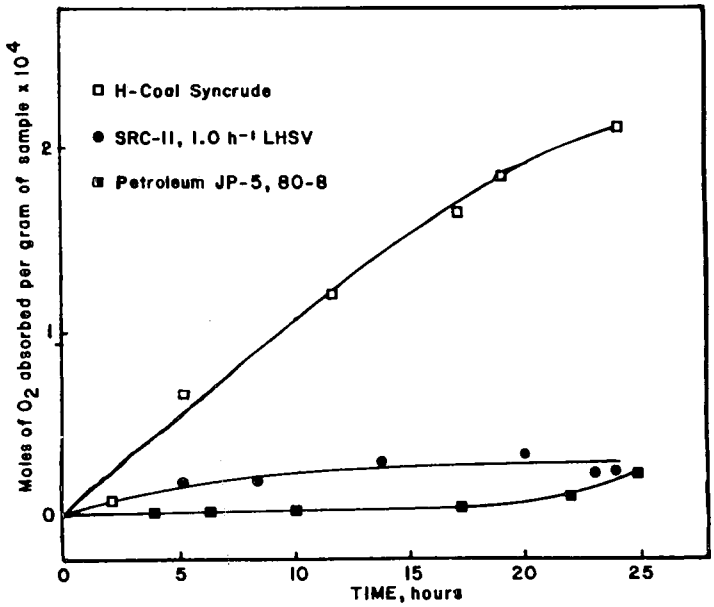

Fig. 2 Oxygen uptake by liquid fuels at 323 K

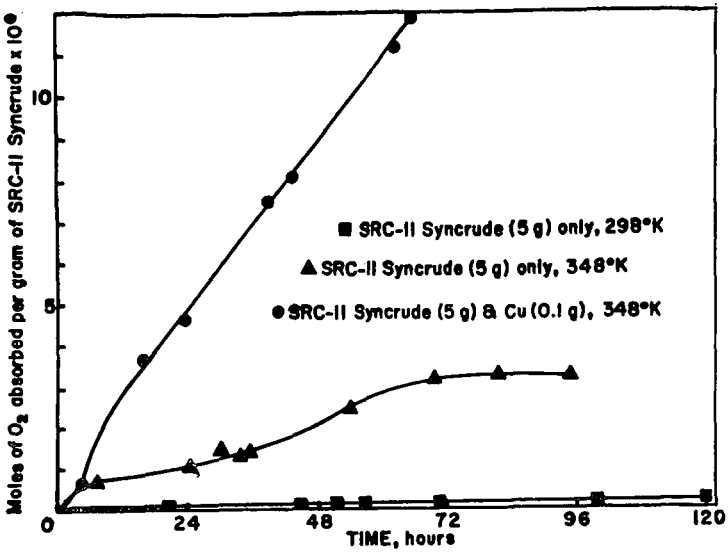

Fig. 3 Oxygen uptake by 5g SRC-II syncrude with and without Cu (0.1g)

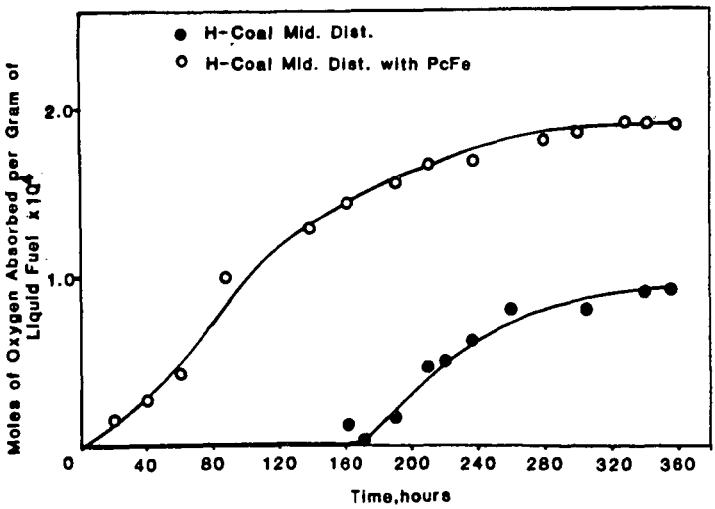

Fig. 4 Oxygen uptake by 5g H-coal middle distillate with and without Pc Fe (0.025g), 296 K

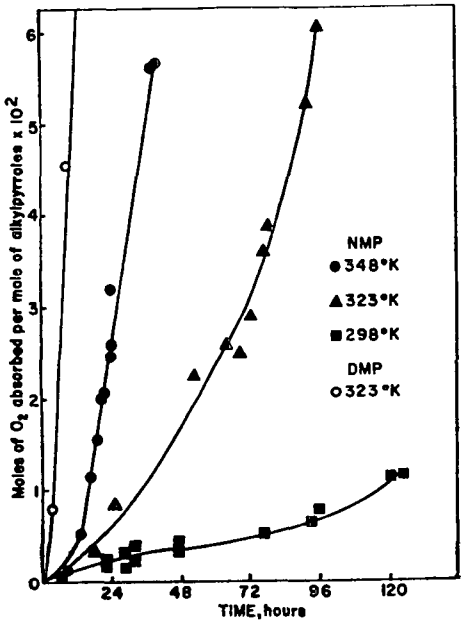

Fig, 5 Oxygen uptake by pure NMP and pure DMP

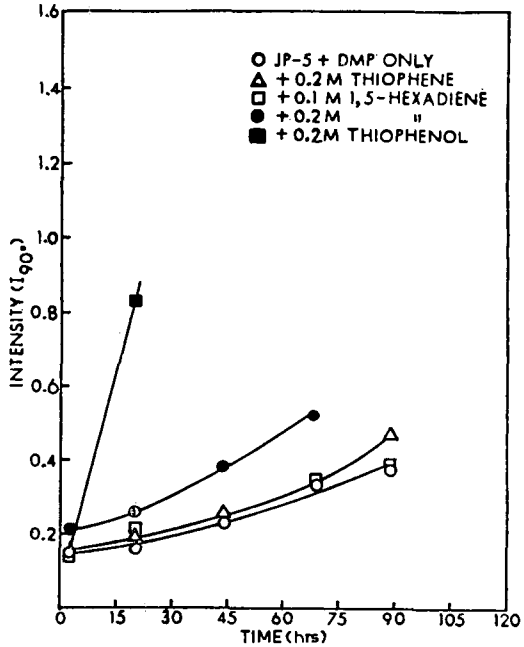

Fig. 6 Light scattering curves for petroleum JP-5, DMP and additives

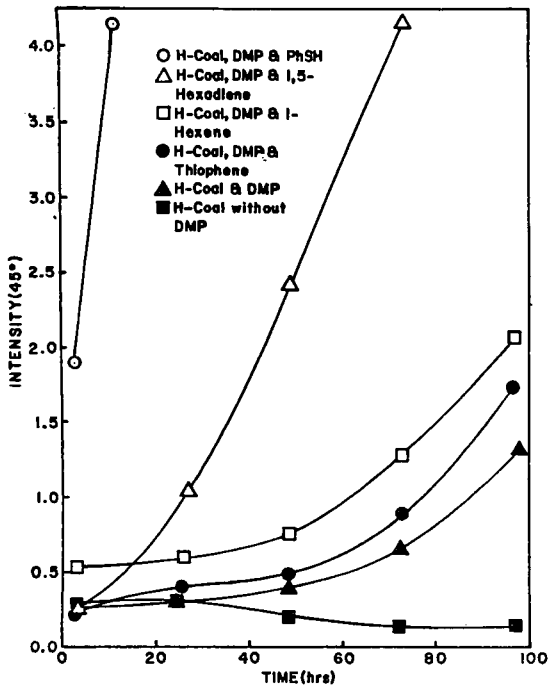

Fig. 7 Light scattering curves for upgraded H-coal (LHSV 0.5) DMP (0.02 M) and additives (each 0.1M)

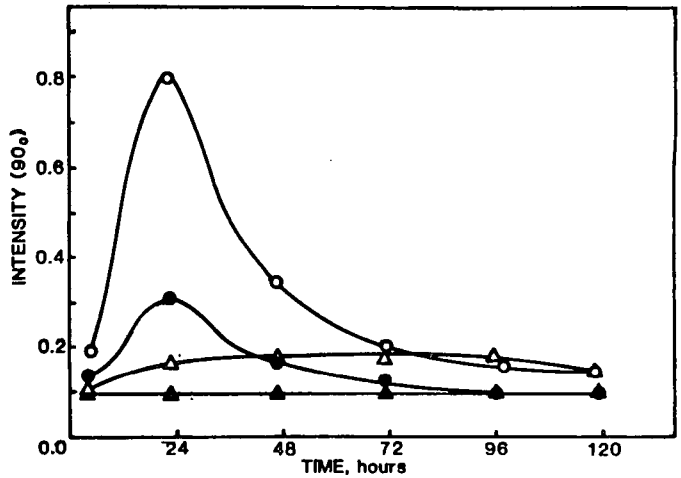

Fig. 8 Light scattering curves for upgraded SRC- II (LHSV 0.5) plus additives:

▲ : 0.036M DMQ only; 0.1M thiophenol only
△ : 3-mercaptopropionic acid (MPA), 0.1M:
● : 0.036 M DMQ + 0.1 M MPA
○ : 0.036 M DMQ + 0.1 M thiophenol

EVALUATION OF OLIGOMERIC MODELS OF COAL ASPHALTENES AND PREASPHALTENES AS GPC CALIBRATION STANDARDS

Richard J. Baltisberger, S.E. Wagner, S.P. Rao, J.F. Schwan and M.B. Jones

Department of Chemistry, University of North Dakota,
Grand Forks, ND 58202

INTRODUCTION

One important facet of the characterization of coal and coal derived materials is that of molecular weight determination. The initial goal of this study was to synthesize a series of model oligomers that were in agreement with the average structural formulas of some selected coal derived asphaltene and preasphaltene samples as determined by proton nuclear magnetic resonance spectroscopy, elemental analyses and various oxygen derivatization procedures. The second goal was to test these model compounds along with some commercially available polystyrene standards as calibration standards for high pressure gel permeation chromatographic procedures. The retention volumes of these model compounds were compared with those volumes for a group of coal derived asphaltene and preasphaltene samples which had been previously isolated by preparative gel permeation chromatographic techniques.

The application of GPC to the characterization of coal derived materials has been studied by a number of researchers (1-13). Coleman et al. (2-3) demonstrated that three column packings; styrene-divinylbenzene (Bio-Beads S-X4), cross-linked poly(acryloylmorpholine), and modified alkylated dextran (Sephadex LH-20) polymers; could be used for the GPC separation of THF and $CHCl_3$ solvent refined coal (SRC) fractions. Schwager et al. (1) isolated four SRC asphaltene fractions by preparative techniques using Bio-Beads SX8. A linear relationship between the logarithm of number average molecular weight and retention volume was observed using an analytical μ-styragel HPLC column. The analytical column was calibrated with a series of aromatic hydrocarbons, a porphyrin and propylene glycols of known molecular weight. Curtis et al. (4) studied the characteristics of an SRC (Amax) using GPC techniques. The separation employed three μ-styragel columns using THF as the solvent and was calibrated with a series of polyethylene glycol and various polynuclear aromatic hydrocarbon standards. Sephadex LH-20 has also been used to fractionate the hexane soluble portion of the pyridine extract from a Sorachi coal (5). Khan (6) compared the use of GPC and vapor pressure osmometry (VPO) to obtain molecular weight data for the hexane soluble portion of three H-coal liquids. Two packings, polyvinylacetate (Fractogel PVC 500) and styrene-divinylbenzene copolymer (Toyo Soda, G2000H10) were used as analytical columns. Calibration of the columns was accomplished by VPO measurement of number average molecular weight in toluene of preparative scale fractions obtained from a Fractogel column.

All of this work has demonstrated that the quantitative interpretation of GPC chromatograms raises two problems. First, the response of the detector must remain constant on a per weight basis over the molecular range (i.e., type and distribution of chromopores must be constant). A constancy of uv absorbance per gram for a series of SRL materials has been reported in work by Ruud (9). However, this point needs to be investigated more thoroughly. A second problem, which is the focus of this paper, is the establishment of the response curve with suitable calibration standards.

EXPERIMENTAL

Materials

Polystyrene standards used to obtain the reference GPC curve were obtained from Polysciences, Inc. Other standard compounds were synthesized from starting materials obtained from various commercial sources (14). Solvent refined lignite (SRL) samples produced at 460°C, 27.6 MPa (4000 psig) using synthesis gas were obtained from the Grand Forks Energy Technology Center and solvent fractionated to obtain asphaltene and preasphaltene fractions (15). The lignite used was from a North Dakota seam, Beulah three.

Preparative Scale GPC

The SRL asphaltenes and preasphaltenes were further separated using a 50 mm id x 120 cm glass column packed with Bio-Beads S-X3 (200-400 mesh) styrene-divinyl benzene. Prior to GPC separation all the SRL samples were acetylated in order to convert the hydroxyl sites to their acetate forms. Freshly distilled toluene or pyridine was used as the solvent. Typical analytical GPC chromatograms of an asphaltene sample obtained from the preparative column are presented in Figure 1. Elemental analyses of the fractions were performed by Spang Microanalytical Laboratory and number average molecular weights were determined in our laboratory using a Wescan Model 117 Vapor Pressure Osmometer. In normal runs, 2-3 concentrations over the range 1 to 50 g/kg of pyridine were employed for extrapolation to infinite dilution.

Analytical Scale GPC

Analytical scale GPC analyses (HPLC) were carried out using three 10 nm and one 50 nm μ-styragel columns in series, with THF (UV grade, Burdick and Jackson) as the mobile phase. A Laboratory Data Control Model 1205 UV Monitor was used as the detector (254 nm) and a Waters Model UK6 injector was used to inject samples of about 10 μl at 10 mg/ml. Samples were filtered across a 0.5 μm millipore filter prior to injection. The flow rate was usually maintained at 1.0 mL/min to prevent pressures in excess of 1000 psig.

RESULTS AND DISCUSSION

The determination of the number average molecular weights of the asphaltene and preasphaltene SRL fractions by vapor pressure osmometry (VPO) makes it possible to establish the experimental relationships between elution volume in the analytical GPC and molecular weight. Band broadening of the peaks as shown in Figure 1 is a function of the number of theoretical plates of the column and the polydispersity of the sample. The column system was found to have 7,500 plates when using pyrene in THF. The polydispersity ratios (M_w/M_n) of the SRL samples were measured using commercial polystyrene for calibration of the molecular weight and retention volumes assuming a linear response. The polydispersity ratio for each of the polystyrene standards was 1.3. The range of polydispersity values of the SRL fractions was found to be 1.05 to 1.3.

Figure 2 shows a plot of the logarithm of molecular weight versus retention volume for the polystyrene standards, the acetylated SRL asphaltenes and preasphaltenes and a series of oligo(aryl ethers) and oligo(aryl methylenes) from 170-570 g/mole. A nearly linear relationship was found provided the aryl moieties were benzenoid. However, deviations from linearity were observed for both model compounds and SRL samples containing more

condensed aromatic nuclei (i.e., naphthalene, phenanthrene and pyrene). Substances containing larger aromatic nuclei were found to elute too late for their molecular weight. The length per molecular weight of these compounds is less than a benzenoid molecule of the same weight. Because of the smaller size these compounds elute at a later time. The fraction of aromatic carbons present as edge carbons (H_{aru}/C_{ar}) was measured by proton nmr to be 0.63 to 0.90 for the asphaltenes and preasphaltenes. Calculated values of H_{aru}/C_{ar} for the model compounds ranged from 0.67 to 1.0 and for the polystyrene standards were 1.0. Those SRL samples with H_{aru}/C_{ar} ratios greater than 0.70 gave nearly a coincident linear plot with the polystyrene standards as shown in Figure 2.

Philip and Anthony (12) have shown that when THF is used as a mobile phase species capable of hydrogen bonding result in elutions corresponding to larger molecular size and smaller retention volumes. We observed this effect particularly for 200-300 g/mole model compounds containing a phenolic hydroxyl group. Philip and Anthony (12) also observed that rigid molecules such as polynuclear aromatics have smaller molecular sizes and thus larger retention volumes. The present direction of our research is to prepare a series of condensed aromatic oligomers so we can better match the H_{aru}/C_{ar} values of the calibration standards and the coal derived liquids.

CONCLUSIONS

Polystyrene, oligo(phenyl ethers) and/or oligo(phenyl methylenes) are suitable GPC calibration standards for most derivatized SRL asphaltenes and preasphaltenes. More condensed aromatic oligomers (i.e., containing phenanthryl and pyrenyl moieties) may be required for accurate GPC determination of the molecular weights of SRL samples with low H_{aru}/C_{ar} (highly condensed aromatics). The SRL samples must be derivatized to block free -OH groups and prevent interaction with the GPC solvent, THF.

ACKNOWLEDGEMENT

The research was supported by DOE through contract number DE-FG22-81PC40810.

REFERENCES

1. Schwager, I.; Kwan, J.T.; Lee, W.C.; Meng, S.; Yen, T.F. Anal. Chem., 1979, 51, 1803-1806.
2. Coleman, W.M.; Wooton, D.L.; Dorn, H.C.; Taylor, L.T. J. of Chromatography, 1976, 123, 419-428.
3. Coleman, W.M.; Wooton, D.L.; Dorn, H.C.; Taylor, L.T. Anal. Chem., 1977, 49, 533-537.
4. Curtis, C.W.; Hathaway, C.D.; Guin, J.A.; Tarrer, A.R. Fuel, 1980, 59, 575-582.
5. Yoshii, T.; Sato, Y. Fuel, 1979, 58, 534-538.
6. Khan, M.M. Fuel, 1982, 61, 553-556.
7. Nomura, M.; Kurosaki, T.; Miyake, M. Chem. Letters, 1983, 329-332.
8. Knudson, C.L.; Schiller, J.E.; Ruud, A.L. In "Organic Chemistry of Coal"; Larsen, L.W., Ed.; A.C.S. Symposium Series, 71; American Chemical Society: Washington, 1978; Chapter 22.
9. Ruud, A.L. M.S. Thesis, The University of North Dakota, Grand Forks, ND, 1979.

10. Wagner, S.E. M.S. Thesis, The University of North Dakota, Grand Forks, ND, 1983.
11. Beilina, N.Y.; Zhidkova, A.F.; Fedotov, M.V. Khimiya Tv. Topliva (Solid Fuel Chemistry), 1983, 17, 93-96 (English Translation).
12. Philip, C.V.; Anthony, R.G. Am. Chem. Soc., Div. Fuel Prepr., 1979, 24(3), 204-214.
13. Wong, J.L.; Gladstone, C.M. Fuel, 1983, 62, 870-872.
14. Baltisberger, R.J.; Jones, M.B. April, 1983, DOE Report DOE/PC/40810-5. Baltisberger, R.J.; Jones, M.B. Sept., 1982, DOE Report DOE/PC/40810-3.
15. Steffgen, F.W.; Schroeder, K.T.; Bockrath, B.C. Anal. Chem., 1979, 51, 1164-1168.

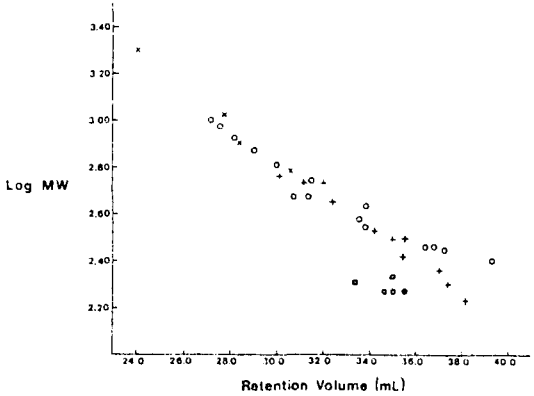

Figure 2. GPC calibration plot. X = polystyrene standards; o = SRL samples with $H_{aru}/C_{ar} \geq 0.70$; + = model compounds with $H_{aru}/C_{ar} \geq 0.89$ and without phenolic -OH; ● = model compounds with $H_{aru}/C_{ar} \geq 0.89$ and with phenolic -OH.

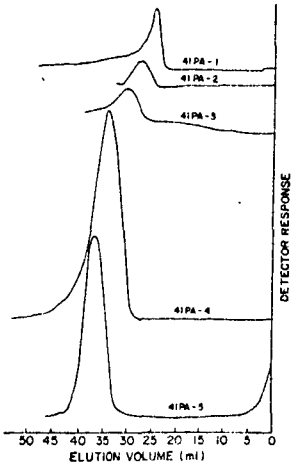

Figure 1. HPLC GPC chromatograms of acetylated SRL preasphaltenes separated by preparative GPC.